TECHNICAL REPORT STANDARD TITLE PAGE

1. Report No.	2. Government Accession No.	3. Recipient's Catalog No.

4. Title and Subtitle	5. Report Date
Methods of Avalanche Control on Washington Mountain Highways - Fourth Annual Report	July 1974
	6. Performing Organization Code

7. Author(s)	8. Performing Organization Report No.
C.B. Brown; R.J. Evans; D.M. McClung; E.R. LaChapelle; and M.B. Moore	

9. Performing Organization Name and Address	10. Work Unit No.
Geophysics Program and Department of Civil Engineering University of Washington Seattle, Washington 98195	11. Contract or Grant No. Y-1301
	13. Type of Report and Period Covered INTERIM July 1973 - June 1974
12. Sponsoring Agency Name and Address Washington State Highway Commission Department of Highways, Highway Administration Bldg. Olympia, Washington 98504	14. Sponsoring Agency Code

15. Supplementary Notes

Co-operation with U.S. Department of Transportation, Federal Highway Administration.

16. Abstract

A collection of reports about avalanche conditions and avalanche prevention measures on Washington mountain highways in general and to the North Cascade Highway in particular, involving various aspects of creep deformation and glide of the snow cover as they affect avalanche defense structure design; reconnaissance of a proposed new highway route through the Cascade Mountains; and a continuing study of the relationship between synoptic winter weather patterns and the formation and distribution of snow avalanches in the Cascades. The reports are entitled:

1. Effect of Glide and Creep on Rigid Obstacles by C.B. Brown and R.J. Evans.

2. Creep and the Snow-Earth Interface Condition in the Seasonal Alpine Snow-Pack by D.M. McClung.

3. In-Situ Investigations of the Temperature Dependence of the Creep of Low Density Snow by D.M. McClung

4. Naches Tunnel Avalanche Reconnaissance by E.R. LaChapelle.

5. Investigation of Synoptic and Surface Weather Situations Leading to Major Avalanche Cycles in the Washington Cascades for the 1973-74 Winter by M. B. Moore.

17. Key Words	18. Distribution Statement
Avalanche, Snow, Weather, Creep, Glide, Avalanche Forecasting	

19. Security Classif. (of this report)	20. Security Classif. (of this page)	21. No. of Pages	22. Price
Unclassified	Unclassified	81	

Form DOT F 1700.7 (8-69)
HWY FORM 341-004 6/72

METHODS OF AVALANCHE CONTROL ON WASHINGTON MOUNTAIN HIGHWAYS

Co-principal Investigators
E. R. LaChapelle
C. B. Brown
R. J. Evans

Geophysics Program and
Department of Civil Engineering
University of Washington

INTERIM REPORT
(Fourth Annual Report)

Research Project Y-1301
Phase IV

Prepared for
Washington State Highway Commission
Department of Highways
In cooperation with
U.S. Department of Transportation
Federal Highway Administration

July 1974

The contents of this report reflect the views of the authors who are responsible for the facts and the accuracy of the data presented herein. The contents do not necessarily reflect the official views or policies of the Washington State Department of Highways or the Federal Highway Administration. This report does not constitute a standard, specification, or regulation.

TABLE OF CONTENTS

INTRODUCTION

This report covers the fourth and final year of activity under a contract intended to develop information about avalanche conditions and avalanche prevention measures on Washington mountain highways in general and to the North Cascade Highway in particular. The scientific studies conducted during fiscal year 1974 are summarized in this report. They deal with various aspects of creep deformation and glide of the snow cover as they affect avalanche defense structure design in the mountain climate of Western Washington, with reconnaissance of a proposed new highway route through the Cascade Mountains, and with a continuing study of the relationship between synoptic winter weather patterns and the formation and distribution of snow avalanches in the Cascades.

Another major activity during the fourth year of this contract was the compilation of an Avalanche Atlas for the Cascade Mountain Passes in the same format as the one compiled in 1971 for the North Cascades Highway. This Atlas is printed in two parts: Part I covers Chinook, Cayuse, White and Snoqualmie Passes; Part II covers Stevens Pass and Tumwater Canyon.

EFFECT OF GLIDE AND CREEP ON RIGID OBSTACLES

by

C. B. Brown and R. J. Evans

ABSTRACT: The forces on a rigid obstacle caused by creep and glide of snow down a slope are provided by a finite element procedure. The element is a trapezium with sides bounded by the snow surface, the snow-ground interface and planes normal to the ground. The problem is treated as one of plane strain but extensions to considerations of three dimensions are discussed. Glide resistance is incorporated as a basal shear dependent on the glide velocity; the snow pack is treated as having a linear non-homogeneous flow law.

Résumé: Les forces exerceés sur un obstacle rigide dues an fluage et au glissement de la neige sur un plan incliné sont calculeés par la méthode des éléments finis. L'élement fini est un trapèze dont deux cotés sont perpediculaires au sol et les deux autres sont, respectivement, suivant la surface de la neige et la surface de contact entre la neige et le sol. Le probleme est traité en un problème de déformations planes mais des considérations relatives à l'extension à un traitement tri-dimensionel sont présenteés. La résistance au glissement est traitée en tant qu'éffort tranchant s'exercant sur la base et dépendant de la vitesse de glissement. La neige est traiteé comme matériau non homogène à loi de fluage linéaire.

Introduction

This paper is concerned with the development of an element which has the special facility of conforming to the snow pack kinematics in neutral zones and the boundary conditions on rigid obstacles. Once developed and included in a finite element solution scheme, forces on rigid obstacles and regimes of creep and glide can be predicted.

The kinematics of creep and glide in neutral zones, that is, where equilibrium exists between the body force acting down the slope and the glide restraint, has been measured by McClung on Mount Baker in the Cascade Mountains. These observations, first reported by Brown, Evans and McClung (1972) and confirmed in McClung (1973) show creep and glide rates to be of the same order

of magnitude. More importantly, the creep profile throughout the thickness is approximately linear. This means that straight lines normal through the thickness translate and rotate to inclined straight lines as shown in Figure 1(a). A similar creep profile has been reported for Swiss Alpine snow by Haefeli (1939).

In calculating forces on rigid obstacles such as snow bridges due to creep and glide, some approximate, or numerical, scheme is necessary. The observed nature of the deformation is utilized here in developing a convenient numerical method to analyze the state of stress and deformation and restraining forces due to creep and glide. Plane sections remain plane, not only as observed in neutral zones, but also at rigid obstacles (x_1=0 in Figure 1(a)). It therefore appears reasonable to base an assumed displacement field on the assumption that plane sections remain plane everywhere throughout the length of the slab. It is this assumption which is used here in developing a finite element procedure.

The first part of the paper outlines the formulation of the problem and the solution procedure. In the remainder of the paper an example is given and the implications of the work are discussed.

Problem Statement and Formulation

Two possible steady creep constitutive laws have been suggested by Brown, Evans and McClung (ibid) to describe observed creep motion; here the more complex non-linear isotropic law is abandoned and the inhomogeneous law is used in which strain rate depends linearly on stress but where the modulus of viscosity varies linearly with depth and is zero at the surface. The snow is assumed to be isotropic with constant Poisson's ratio and hence shear viscosity varies linearly, also being zero at the surface.

For slow (quasi-static) motion, the field equations consist of the stress equations of equilibrium, the stress-strain rate (constitutive) equations and the strain rate-velocity equations. For plane motion (referring to Figure 1) boundary conditions are:

a) at x_2=h, surface traction is zero.

b) at x_2=0, the normal velocity is zero; tangential traction is related to tangential velocity by the glide law.

c) at x_1=0, normal velocity is zero, tangential velocity is either zero

or related to tangential traction by a glide law.

d) the extent of snow cover up the slope is taken into the neutral zone and the upper boundary may be considered to be traction free.

The problem is thus equivalent to one of a linearly elastic body provided that the total times are short enough for overall geometry changes to be ignored; the kinematic variable is velocity rather than displacement.

Solution methods of the theory of elasticity may be used and in general approximate solution schemes are required. Bucher (1948) employed an approximate analytic scheme but, in general, the finite element method suggests itself. Several programs are available, particularly for plane problems: McClung (ibid), for example, has made use of such a program.

The element used here extends the full depth of the pack and is derived for deformation restricted to be plane. Only lateral (x_1 direction) motion is considered, any settlement analysis and resulting tangential force on obstacles may be considered separately without inducing serious error in the analysis of downhill motion.

Element Stiffness Matrix

The rectangular element employed for regular geometry such as shown in Figure 1(a) is shown in Figure 2. For irregular geometry such as shown in Figure 1(b) a rhombic element is required. The stiffness matrix for such a rhombic element is given in the Appendix. Methods of calculation for stiffness matrices are now well documented (Zienkeiwicz and Chang, 1967). Matrix computations will not be described here. For the generalized velocities U_1 through U_4 as shown in Figure 2 the stiffness matrix is

$$[K] = E_0 H \begin{vmatrix} 1 & -\frac{1}{6} & -1 & \frac{1}{6} \\ -\frac{1}{6} & \frac{1}{12}(1+\frac{4a}{H^2}) & \frac{1}{6} & \frac{1}{12}(-1+\frac{2a}{H^2}) \\ -1 & \frac{1}{6} & 1 & -\frac{1}{6} \\ \frac{1}{6} & \frac{1}{12}(-1+\frac{2a}{H^2}) & -\frac{1}{6} & \frac{1}{12}(1+\frac{4a}{H^2}) \end{vmatrix} \qquad (1)$$

Where L is the element length, $H = \frac{h}{L}$, $a = \frac{1}{2(1-\nu)}$, ν is Poisson's ratio and E_0 is the modulus at $x_2=0$. E_0 is taken to be a linear function of the mean hydrostatic stress for the element.

Glide Stiffness Matrix

Following Brown, Evans and McClung (ibid.) and McClung (ibid.) a linear glide law of the form.

$$\tau = \beta u \tag{2}$$

is used where τ is the basal shear, u is the basal velocity and β is a constant. From (2) and employing the coordinates of Figure 2, the glide stiffness matrix is

$$[K_g] = \frac{\beta L}{3} \begin{vmatrix} 1 & -\frac{1}{2} & \frac{1}{2} & -\frac{1}{4} \\ -\frac{1}{2} & \frac{1}{4} & -\frac{1}{4} & \frac{1}{8} \\ \frac{1}{2} & -\frac{1}{4} & 1 & \frac{1}{2} \\ -\frac{1}{4} & \frac{1}{8} & \frac{1}{2} & \frac{1}{4} \end{vmatrix} \tag{3}$$

Body Force

The generalized body force matrix for an element is

$$\{F\} = \frac{1}{2}\rho g \sin\gamma\, hL \begin{vmatrix} 1 \\ 0 \\ 1 \\ 0 \end{vmatrix} \tag{4}$$

where ρ is the mass density and γ is the slope angle.

Example

A plane strain solution is presented here for a snow pack of uniform depth, infinite in extent upslope from a rigid wall whose upslope face is perpendicular to the slope. Snow data and properties used are those measured by McClung (ibid.) at Mount Baker and hence may be considered to be typical for the Cascade Mountains.

The following data are used:

$h = 3.6$ m., $\rho g = 546$ kg/m^3, $\gamma = 45°$

For these values, McClung (ibid.) measured neutral zone glide and creep velocities of 1.50×10^{-8} m./sec and 0.66×10^{-8} m./sec. For $\nu = .3$, these data

correspond to

$$E_o = 1.37 \times 10^{12} \quad \text{NT sec/m}^2$$

$$= 9.26 \times 10^{11} \quad \text{NT sec/m}^2$$

Results presented are shown for the element layout shown in Figure 3. Member displacements and forces are calculated; shown here are the basal velocity distribution and also the resultant force and moment on the restraining structure. The basal velocity is shown in Figure 4 while the forces acting on the structure per meter width at $x_2 = \frac{h}{2}$ are

$$\text{Force} = 6.07 \times 10^4 \quad \text{NT (downslope)}$$

$$\text{Moment} = 1.39 \times 10^4 \quad \text{NT (clockwise)}$$

McClung (ibid) has carried out a detailed finite element analysis of the same problem so some comparison is possible. McClung's basal velocity distribution is shown in Figure 4. His stress distribution results in the following actions on the restraining structure:

$$\text{Force} = 6.83 \times 10^4 \quad \text{NT}$$

$$\text{Moment} = 1.29 \times 10^4 \quad \text{NT m}$$

General agreement with the detailed finite element solution is seen to be quite good; some comment on the solution procedure is merited.

Numerous element sizes have been used for this problem and the solution, particularly the displacements, appears to be relatively insensitive to element size provided that several are used to span the back pressure zone. In the neutral zone, of course, the assumed displacement field is exact and any length element may be used. The use of the very short element adjacent to the restraining structure is to permit computation of forces there. For longer elements, these forces contain a contribution due to differential glide.

Both E_o and β were assumed to depend linearly on mean hydrostatic stress. This required an iterative solution scheme since this stress is not known a priori. Neutral zone values were used initially and subsequently revised from computed stress values. For all problems solved to date, two or three iterations have sufficed to give convergence.

Discussion

The element developed here possesses the observed kinematic features in the neutral zone and at the rigid obstacle. In the intermediate zone there is no evidence that creep varies linearly. This suggests that experiments in this zone could be valuable in attesting to the validity of this work. McClung (ibid.) obtains a nonlinear velocity profile in the intermediate zone by the use of conventional finite element analysis. However, without experimental evidence such deformations are no more valid than the linear form utilized here.

In Brown, Evans and McClung (ibid.) two constitutive laws were proposed to account for the observed motions in the neutral zone. The simpler one has been incorporated into this work and yet no real evidence is available concerning the merits of either development. Both simulate the observed kinematics; the use of non-homogeneous modulus is attractive for its simplicity but again a full justification would require further experimentation in the intermediate zone.

These comments suggest that the proposed element appears to incorporate existing observations satisfactorily. In the work of Haefeli (ibid.) an additional force facet is included, namely the static pressure developed by the snow against the rigid obstacle. In this paper only body force creep against the obstacle is included. During deposition of snow, a state of stress will develop in the pack due to incremental loading by the acceleration process. For the elastic case, these stresses have been given by Brown, Evans and LaChapelle (1972) and they give rise to a lateral force per unit width on a rigid restraining structure given by

$$F = \frac{1}{2} \frac{\nu}{1-\nu} \rho g H^2 \cos\gamma \qquad (5)$$

For the present case, the force would also be given by (5) where symbols are as previously defined. This is because, although self equilibrating states of stress disappear in the time due to relaxation (King, 1955), the accretion forces are in equilibrium with the applied body force and thus are not self equilibrating. The force given by (5) for the constants used previously is 1.09×10^4 NT which should be added to the force given above to obtain the total force on the barrier.

It should be noted, however, that the analysis presented in this paper

is applicable to anisotropic viscous behavior provided ν is not necessarily interpreted as Poisson's ratio. The glide and creep solution is not, in fact, particularly sensitive to Poisson's ratio. It is reasonable to suppose that the constant ν in (5) can vary anywhere from 0 to .5 regardless of the previous solution and hence the force due to accretion is bounded between 0 and 2.5×10^4 NT.

The simple element proposed in this paper can be easily extended to deal with non-uniform thickness snow in the manner given in the Appendix. Additionally, the expansion of the plane element into a parallelepiped with sixteen generalized co-ordinates is completely consistent with the development in this paper. In such a situation the three-dimensional analysis of snow on avalanche slopes can be undertaken without incurring computer capacity problems. The glide and creep down and across the slope, together with rigid obstacles scattered on the slope can be included in such a model. This removes the restriction of plane strain evident in existing work and yet provides a solution where neither plane strain nor plane stress exists. It is believed that a practical value for such an approach in avalanche defense analysis exists.

In the example presented here, the information obtained would certainly be as effective for defense design as more detailed finite element procedure. Forty generalized coordinates were used in comparison with some 300 for the latter procedure used by McClung.

In conclusion, it might be noted that the force calculated is in reasonable agreement with that predicted by the Swiss Guidelines for comparable glide and creep factors. The guidelines, of course, do not predict a moment.

References

Brown, C. B., Evans, R. J., and LaChapelle, E. R., 1972. Slab Avalanching and the State of Stress in Fallen Snow, Journal of Geophysical Research, Vol. 77, p. 4570-4580.

Brown, C. B., Evans, R. J., and McClung, D., 1972. Incorporation of Glide and Creep Measurements in Snow Slab Mechanics, Advances in North American Avalanche Technology; 1972 Symposium, p. 7-13.

Bucher, E., 1948. Contribution to the Theoretical Foundations of Avalanche Defense Construction, Translation 18, S.I.P.R.E., February, 1956.

Haefeli, R., 1939. Snow Mechanics with References to Soil Mechanics. Snow and its Metamorphism, Chapter II., Translation 14, S.I.P.R.E., January 1954, p. 57-218.

King, I.P., 1965. Finite Element Analysis of Two-Dimensional Time-Dependent Stress Problems. Structures and Materials Research Report No. 65-1, Structural Engineering Laboratory, University of California, Berkeley.

McClung, D., 1973. Avalanche Defense Mechanics, Ph.D. Dissertation, University of Washington, Seattle.

Zienkeiwicz, O. C. and Chang, Y.K., 1967. The Finite Element Method in Structural and Continuum Mechanics, McGraw-Hill.

APPENDIX

A plane strain element to incorporate the geometry of Figure 1(b) will be rhombic in shape. Generalized co-ordinates of $\bar{U}_1$, $\bar{U}_2$, $\bar{U}_3$, $\bar{U}_4$ are shown in Figure A. The modulus, E, is zero at the top surface and increases linearly at Δ to the bottom surface. The 4 x 4 stiffness matrix then has the following element values:

$$k_{11} = k_{33} = -k_{13} = -k_{31} = \frac{\Delta}{6L} \{3hF + h_1^2 + B(A+B)\}$$

$$k_{12} = k_{21} = -k_{23} = -k_{32} = \frac{\Delta}{24L} \{h_1^2 C - 2h^3 - B(2hA + 3CB - 2B^2)\}$$

$$k_{14} = k_{41} = -k_{34} = -k_{43} = -\frac{\Delta}{12L} \{D(3hF + h_1^2) + AB(D-2h) + B^2(D-4h - \tfrac{3}{2}h_1) - B^3 + \tfrac{1}{2}h_1^3 - h^2(3h_1+4h)\}$$

$$k_{24} = k_{42} = \frac{\Delta}{120L} \{\tfrac{5}{2}D(2h^3 - h_1^2 C) + 5hB(DA-hJ) + \tfrac{5}{2}B^2[3DC=h(16h+9h_1)] + B^3(5D-25h-8h_1) \cdot 6B^4 - 5h^3C - \frac{h_1^3}{2}(4h_1+5h) + kL^2[3h_1^2+10hF+B(6h_1+25h) + 3B^2]\}$$

$$k_{22} = \frac{\Delta}{120L} \{5FGh + 2h_1^4 + 15h^3B + 5hB^2(3h_1+5h) + 4B^3(2h_1+5h) + 6B^4 + kL^2[2h_1^2 + 10hC + B(4h_1-5h) + 2B^2]\}$$

$$k_{44} = \frac{\Delta}{120L} \{5D^2(h_1^2+3hF) + 5D[h_1^3-2h^2(3h_1+4h)] + 2h_1^4 + 10h^3A + 5B[AD(D-4h)+6h^2C] + 5B^2[6hC+D(3D-3h_1-8h)] + 2B^3[4h_1+5(3h-D)] + 6B^4 + kL^2[12(h_1^2 + B^2) + 10h(2h_1+2h) + 3B(8h_1+5h)]\}$$

Here $A = (2h+2h_1)$, $B = (h_2-h)$, $C = (2h+h_1)$, $D = (h_2-h_1)$, $F = (h+h_1)$, $G = (h^2+h_1^2)$ and $J = (h_1+3h)$. When the geometry of Figure A becomes the element rectangle of Figure 2, then $h_1 = 0$, $h_2 = h$, $\Delta = \frac{-E}{h}$, $A = J = 3h$, $B = 0$, $c = 2h$, $D = F = H$ and $G = h^2$. Using the generalized co-ordinates of the main paper namely

$$U_1 = \bar{U}_1,\ U_2 = \bar{U}_2 h,\ U_3 = U_3,\ U_4 = \bar{U}_4 h$$

then the rhombic stiffness degenerates to (1).

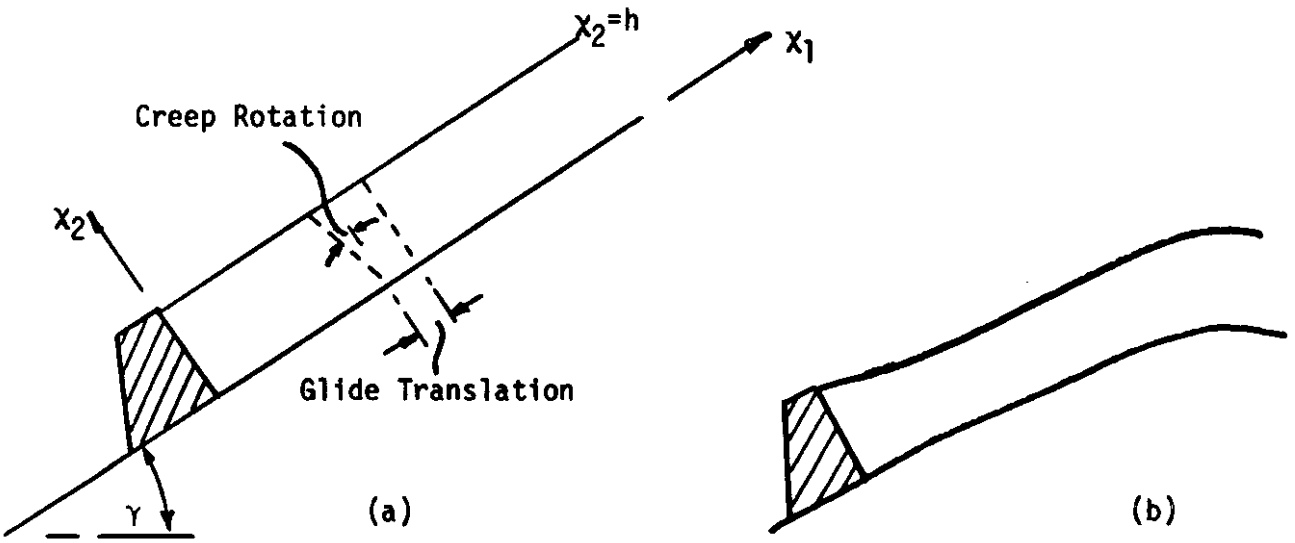

Fig. 1

SNOW PACK GEOMETRY

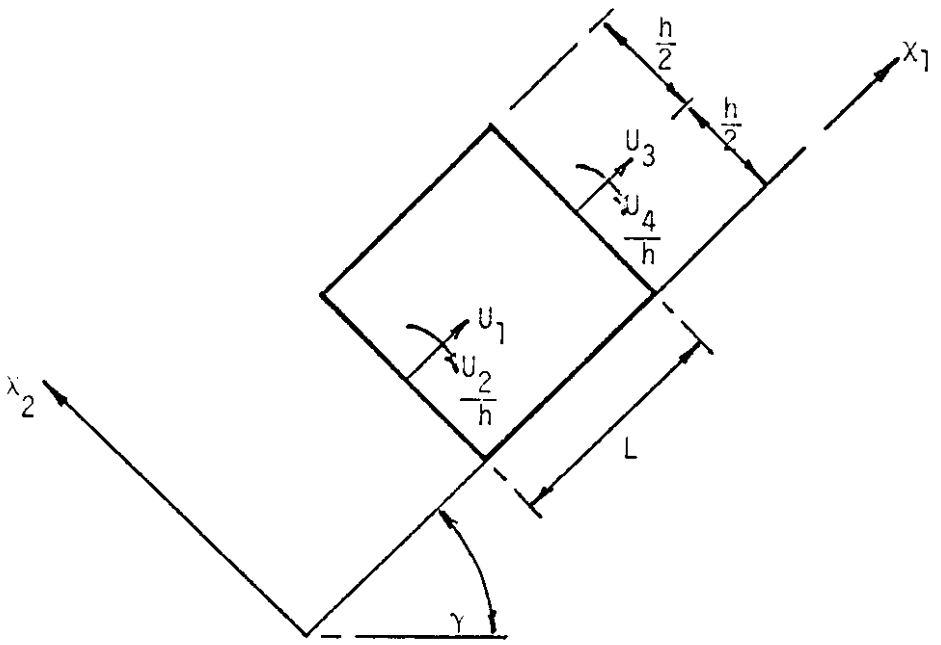

Fig. 2

FINITE ELEMENT

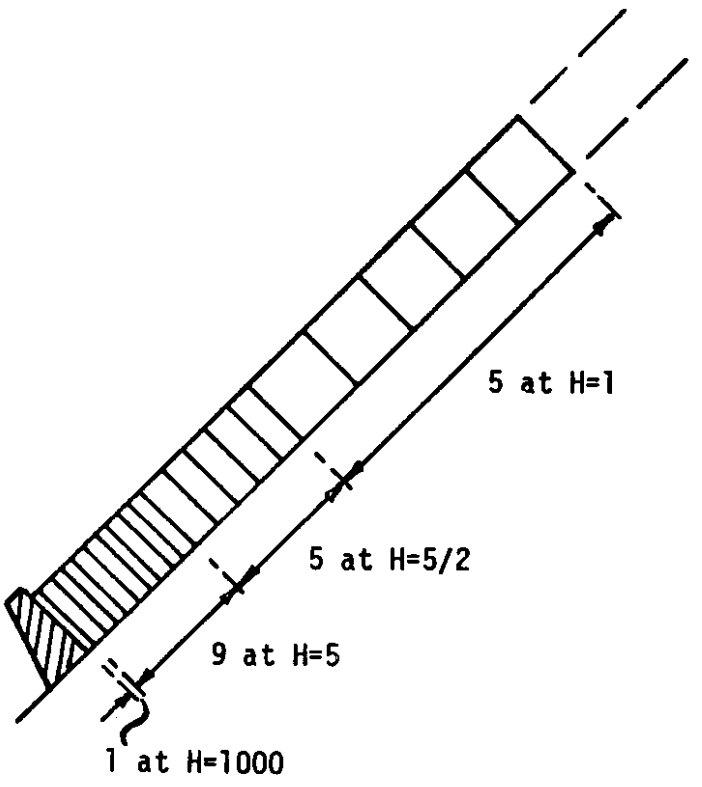

Fig. 3

ELEMENT LAYOUT

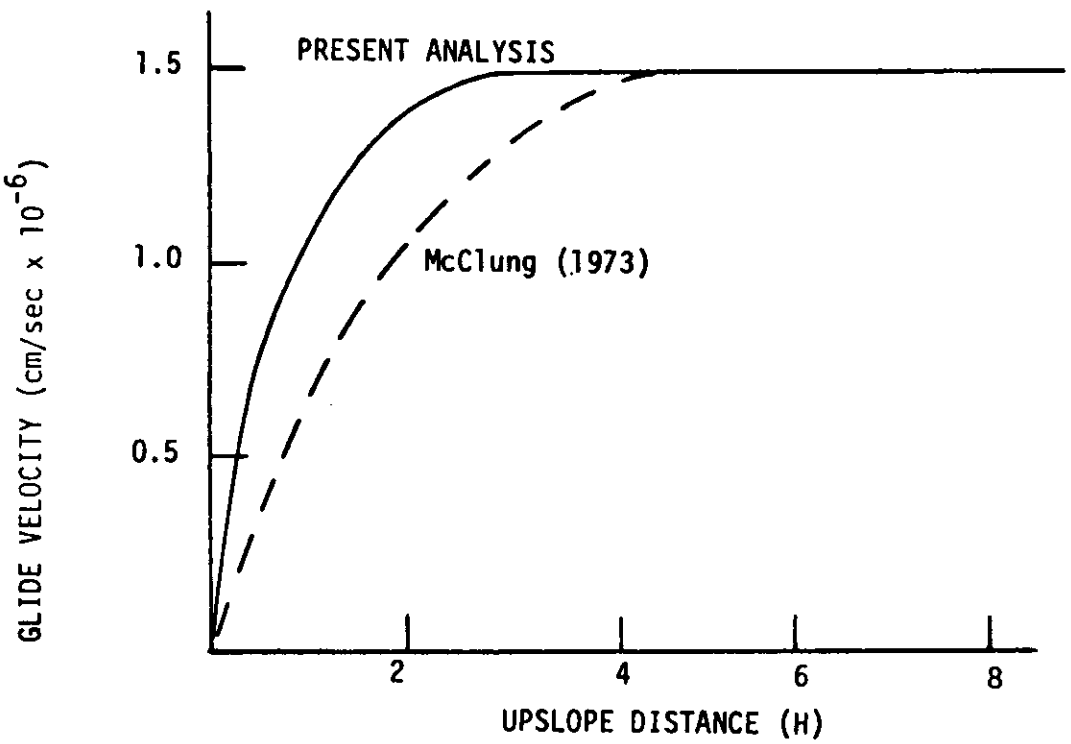

Fig. 4

GLIDE VELOCITY

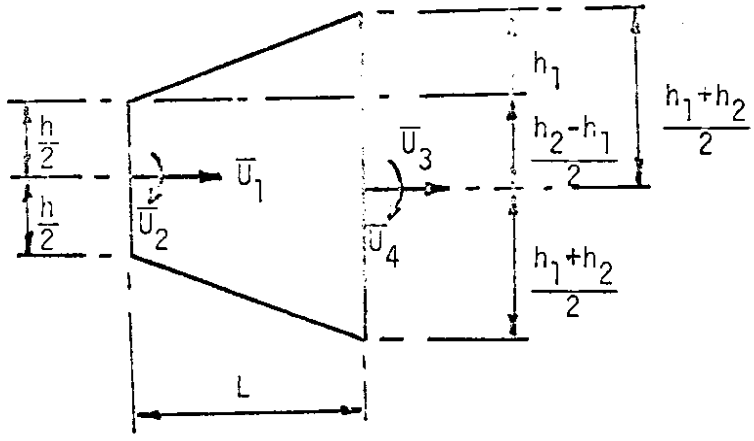

Fig. A

TRAPEZOIDAL ELEMENT

CREEP AND THE SNOW-EARTH INTERFACE CONDITION IN THE SEASONAL ALPINE SNOW-PACK

By David M. McClung

Introduction

When a rigid obstacle is present on a snow-covered slope, the fundamental processes of slow viscous motion are interrupted resulting in a pressure exerted upon the obstacle. In order to formulate problems of snow pressure analytically or numerically, it is essential that the constitutive laws be known relating deformation to stress and relating the shear stress at the base of the snow-pack to the glide velocity.

1. Creep of well-settled, well-metamorphosed, isothermal snow.

Well-settled, well-metamorphosed snow is generally found in the form of well-rounded almost spherical grains in springtime. During the last half of the snow season, the snow-pack is generally isothermal on the lower western slopes of the Cascade Mountains so that the effects of temperature gradients are absent.

Well-metamorphosed seasonal snow is always creeping and densifying under internal body weight stresses. Grains achieve close packing by slowly settling. The density of a random closely packed system of spheres is about 0.58 which is approximately the maximum density of snow which can be found in the seasonal snow-pack, excluding cases where excessive free water is present.

Deviatoric or shear creep of snow seems to call for individual grains to slide by one another. If the grains are modeled as elastic spheres, close packing would imply rather large stress concentrations at grain contact points. If the grains undergo viscous deformation, the stress concentrations would aid the creep process. In either case, if shear creep is modeled as a sliding process, it seems reasonable that the effect of an increase in overburden would be to inhibit the sliding process.

Experiments were performed in the Cascade Mountains during the winters of 1971-72 and 1972-73 on the creep of well-settled, well-metamorphosed, isothermal snow. These experiments were performed in neutral zones by the traditional method pioneered in Switzerland (Bader and others, 1939). The

deformation of sawdust columns was used to define the shear component of creep. Displacement of height markers in the columns was used to define the vertical component of creep. These experiments showed that both the shear strain-rate and the vertical strain-rate are approximately independent of depth in the neutral zone. Figure 1 shows a comparison of the measured shear strain-rates with the results of previous investigators. Density profiles taken concurrently with the creep experiments showed that the density was nearly homogeneous with depth in the late season. If these experiments are interpreted in terms of a non-linear two parameter constitutive law, the apparent implication is that both the shear viscosity and the bulk viscosity are stress dependent.

Consider a two parameter constitutive equation:

$$\dot{\varepsilon}_{ij} = \phi_1 \delta_{ij} + \phi_2 \sigma_{ij} \qquad (1)$$

A similar equation was used by Salm (1967) in an attempt to interpret laboratory triaxial data. ϕ_1 and ϕ_2 must be invarient with respect to proper orthogonal coordinate transformations.

For the shear component,

$$\dot{\varepsilon}_{12} = \phi_2 \sigma_{12} \qquad (2)$$

This equation is satisfied most simply if ϕ_2 is inversely proportional to the hydrostatic stress or equivalently if one defines a shear viscosity proportional to the hydrostatic stress. This possibility was first mentioned by Mellor (1968).

The equation for the vertical component is most simply satisfied if $\phi_1 = K_o$ in the neutral zone.

Therefore, an equation which fits the neutral zone data is:

$$\dot{\varepsilon}_{ij} = K_o \delta_{ij} + \frac{1}{K I_1} \sigma_{ij} \qquad (3)$$

where I_1 is the first invariant of the stress tensor.

This equation may be rewritten:

$$\sigma_{ij} = K I_1 \dot{\varepsilon}_{ij} + K_1 I_1 \delta_{ij} \qquad (4)$$

Summing the diagonal components and rewriting provides a generalization to non-neutral zone situations:

$$\sigma_{ij} = K I_1 \dot{\varepsilon}_{ij} + \frac{I_1}{3} (1 - K J_1) \delta_{ij} \qquad (5)$$

where J_1 is the first invariant of the strain-rate tensor.

By analogy to the constitutive law for a linear compressible viscous solid, the shear and bulk viscosity may be defined respectively:

$$\mu = \frac{KI_1}{2} \qquad \text{and} \qquad \eta = \frac{I_1}{3J_1} \tag{6}$$

The viscous analog of Poisson's ratio may be defined:

$$\nu = \frac{1}{2}\ \frac{1-KJ_1}{1+\frac{1}{2}KJ_1} \tag{7}$$

Figure 2 shows typical neutral zone values of the shear and bulk viscosity with depth calculated from experimental data in the Cascades. Table I lists calculated values of the viscous analog of Poisson's ratio. The viscous analog of Poisson's ratio is constant through the depth of the snow-pack in the neutral zone because J_1 is constant in the neutral zone.

J_1 is physically dependent upon the amount of accumulated settlement and the state of metamorphism of the snow. As time progresses, J_1 slowly approaches zero corresponding to an increase in the viscous analog of Poisson's ratio with time.

In connection with the above remarks, it should be pointed out that the simplest treatment consistent with neutral zone measurements has been utilized. Snow in the seasonal snow-pack is never in a steady state condition and, in addition, it may not be isotropic. These complications represent formidable obstacles to a general approach to creep. Clearly, other combinations of the invariants of the stress tensor could have been produced to match the neutral zone measurements. The approach taken here has been to formulate the simplest theory consistent with the measurements.

2. The interface condition in the seasonal alpine snow-pack: descriptive aspects.

Modeling the slip of a viscous snow-pack over a bed of organic material is expected to be a very complex problem which may never be fully understood.

A series of glide experiments were conducted over the winters of 1971-72 and 1972-73 in the Cascade Mountains. These experiments employed glide strain gauges of the type discussed by in der Gand and Zupancic (1966).

Glide measurements in the form of accumulated strain were taken over regular intervals throughout the snow season at a variety of sites with various slope angles, terrain roughnesses, snow depths and compass attitudes. Temperature measurements accompanied the glide measurements in the form of temperature profiles through the snow-pack taken with a portable temperature probe and in the form of thermistors buried a few centimeters beneath the earth interface. These measurements resulted in the following descriptive aspects of glide:

(1) Glide may be fast at the beginning of the season concurrent with ground temperatures above freezing due to stored summer heat (Figure 3).

(2) The presence of the liquid phase in the form of rain or melt water has profound effects upon the rate of glide (Figure 3).

(3) Glide velocities can fluctuate considerably at any time of the year.

(4) There is no apparent glide when the interface temperature is below freezing.

(5) Increase in glide velocity with increasing snow depth is very difficult to discern because the glide velocity is very sensitive to the local conditions at the interface. Figure 4 shows a possible dependence upon snow depth for two different seasons on a timbered slope. It is possible that the timber exerts a stabilizing influence upon the snow cover making the glide less dependent upon the local interface conditions.

(6) The effect of increased roughness is to slow down the glide process.

(7) The usual situation in the Cascades consists of a layer of well-settled isothermal snow gliding over the ground with the temperature of the ground slightly above 0°C.

3. The physics of snow gliding.

The question of how a viscous body slides over its bed is a very important one in geophysics. It is one of the most important problems in the dynamics of temperate glaciers. In snow mechanics, it is a problem of great practical importance because snow gliding is an important component to snow pressure.

The physical and mathematical theory is much more advanced in relation to the sliding of a glacier over its bed than is the analogous problem of snow gliding over the ground. There are, however, many similarities between the two problems. Accordingly, it seems worthwhile to attempt

application of the ideas of glacier sliding theory to snow gliding.

The theory of glacier sliding [Weertman (1964), Nye (1969), Kamb (1970)] as it now exists attributes the slip of a glacier over its bed to two competing mechanisms: (1) regelation or pressure melting on the uphill side of bed obstacles with subsequent refreezing on the downhill side, (2) creep around the obstacles.

To begin with, it seems worthwhile to consider some obvious differences between the two problems: (1) snow has a much lower viscosity than ice, which allows the creep mechanism to proceed easier than for ice for a given state of stress, (2) stresses at the bottom of the seasonal snow pack are far less than they would be at the bed of a typical glacier and they may not be of sufficient magnitude to drive the regelation mechanism. (3) On the other hand, snow is a granular material and there are presumably stress concentrations at points where grains contact the interface which would tend to make the regelation mechanism easier. Regelation has not been investigated for snow so that relatively little may be stated about the quantitative importance of possible stress concentrations at contact points. (4) The regelation process as envisioned in glacier sliding does not have a strict analog for the snow gliding problem. A porous granular medium such as snow gliding over a bed of organic material is not expected to be modeled exactly like the motion of solid ice everywhere in contact with a solid bed of rock.

As a starting point, consider a quantitative description of snow gliding over ground of a given roughness. The snow is envisioned to be separated from the bed by a thin water film. This water film is deemed to be produced by melting at the base of the snow pack. This is consistent with temperature measurements in the Cascades and with observations in Switzerland [in der Gand and Zupancic (1966)] that observable quantities of snow are melted each year at the base of the snow pack.

The thickness of the water layer envisaged here is just enough to wet the interface, but not thick enough to drown roughness obstacles. This assumption is not essential to the theory presented here, but it is taken as a reference situation providing tractable boundary conditions. If, for example, the interface was only partly wetted, the thin film solution might be viewed as an upper bound. On the other hand, if the water layer were

thick enough to drown roughness obstacles, the thin film solution would be a lower bound. The assumption of a very thin water film, however, seems to be a good physical assumption for steady thermal conditions at the interface.

The snow rheology is assumed to be modeled by an imcompressible Newtonian viscous fluid. In view of the results in the discussion on creep, this assumption is not strictly true since snow is neither linear, nor imcompressible. The consequences of this assumption will be discussed below.

A water film at the base of the snow pack implies that shear stresses cannot be supported there. The normal body weight stresses at the base of the snow pack are then taken to be supported by the roughness obstacles there. The down-slope projection of this normal stress is equivalent to an average shear stress. A relationship between this average shear stress, $<\tau_{xz}>$ and the glide velocity is sought.

The ground roughness is assumed to be modeled by a simple sine wave. A general solution for any model of ground roughness may be obtained by a suitably defined superposition rule. Nye (1970) has obtained solutions for more complicated bed geometries.

For either the creep or regelation mechanisms, analytic solutions are available. Figure 5 defines the symbols and the coordinate system. This problem has been treated by Kamb (1970), Nye (1969), and by W. D. Harrison (unpublished). Nye's nomenclature is followed here.

For the creep mechanisms Nye's solution gives:

$$U_0 = \frac{<\tau_{xz}>}{\mu A^2 K_0^3} \qquad (8)$$

where A is the amplitude of the roughness obstacle (sine wave), $K_0 = \frac{2\pi}{\lambda_0}$ is the wave number, and μ is the shear viscosity.

The regelation mechanism consists of pressure melting on the uphill side of the obstacle with subsequent refreezing on the downhill side. This amounts to a heat flow problem which Nye (1969) has also solved. The solution is:

$$U_0 = \frac{4<\tau_{xz}> CK}{A^2 L K_0} \qquad (9)$$

where K is the mean of the thermal conductivities of snow and the bed

material, L is the latent heat of fusion per unit volume, and C is the slope of the pressure-temperature diagram at the phase transition. C has not been measured for the states of stress found in snow and, in addition, the stresses in a matrix of snow particles are unknown. These factors make it difficult to quantitatively evaluate the effect of regelation in the gliding process.

For the two mechanisms the velocity may be written:

$$U_o = \frac{\langle \tau_{xz} \rangle}{\mu A^2 K_o} \left(\frac{1}{K_o^2} + \frac{1}{K_*^2} \right) \qquad (10)$$

where $K_*^2 = \frac{L}{4CK\mu}$

To compare the importance of the two mechanisms, K_*^2 should be compared to K_o^2. If $K_o^2 << K_*^2$, for example, the drag on the snow pack is determined by the creep mechanism.

It is interesting to compare the value of K_*^2 for snow versus that for ice. It is known that K_*^2 is comparable to or less than K_o^2 for ice in most cases. L will have the same value for snow as ice because snow is composed of grains of ice. For snow of density 500 Kg/m^3 the viscosity is less than that for ice by approximately a factor of 200.

The thermal conductivity of dry snow (density 500Kg/m^3) is less than that for ice. Here, however, concern is with a wet layer of isothermal snow at the base of the snow pack. Sulakvelidze (1954) has reported that wet snow has a conductivity two to three times as high as that of dry snow. Movement of saturated air and migration of liquid water are attributed as contributing to the heat transfer efficiency. Therefore, it appears that the conductivity of wet snow is about the same as that for ice.

The important unknown is the constant C. This parameter would be very difficult to measure for snow.

On the basis of this discussion, the value of K_*^2 is higher by a factor of 200 for snow versus ice by virtue of lower viscosity. On the other hand, it is possible that this factor might be made up for somewhat by the value of C for snow.

Another interesting feature of the problem has been pointed out by Nye (1969). Consider a quantity D defined by:

$$D = \frac{1}{A^2 K_0} \quad \frac{1}{K_0^2} + \frac{1}{K_*^2} \qquad (11)$$

The shear stress may be related to the glide velocity by:

$$\langle \tau_{xz} \rangle = \frac{\mu U_0}{D} \qquad (12)$$

D has a simple geometrical and physical meaning. In Figure 6, D is the depth below the surface at which the averaged velocity profile meets the z axis. D is termed the stagnation depth. The process might be viewed as a rotation around the point P. D is independent of the shear stress, the viscosity and the velocity. D depends only on the topography of the bed. For example, if another geometrical form had been chosen for discussion, $\langle \tau_{xz} \rangle$ would still be proportional to μU_0 but the form of D would change. By decomposing the bed into harmonics, the velocity contribution from each mechanism can be obtained and superposed for each harmonic to get the value of D in the general case.

D characterizes the bed topography. By comparing the magnitude of D with the snow depth for steady mechanical and thermal conditions, it is possible to say something about the mechanism of glide. If D is small compared with the snow depth, the glide motion is mostly by local creep. If D is large with respect to the snow depth, the motion is mostly by regelation. If D is comparable to the snow depth, the motion is shared by the mechanisms. Nye (1969) pointed this out in connection with the glacier sliding problem.

With the knowledge of D as a fundamental measurement in the neutral zone, stagnation depths were measured in the Cascade Mountains during the spring of 1972 and 1973. Table II shows a list of the values of D. Typical snow depths in these areas were at least several meters as compared with typical stagnation depths of tenths of meters. Values of D were calculated from sawdust column experiments performed on the same slopes on which glide measurements were conducted. This is particularly convenient in the case of snow because the averaged velocity profile is a straight line.

In all cases it was found that the values of D are much less than the snow depth for steady mechanical and thermal conditions. Therefore, it seems that the mechanism for glide is local creep around obstacles with regelation playing a very small role if any. The physical reasons are

mainly that snow has a low viscosity making the creep mechanism fast and the comparatively low stresses in the seasonal snow pack are not enough to drive the regelation process.

In the widest definition, the stagnation depth depends not only on the topography of the ground but also on the condition of the interface. For example, if the snow pack had a layer of water which became comparable to the roughness obstacles at the bottom, the situation would be equivalent to a change in topography. The glide measurements show that the velocity is very sensitive to the interface condition so that the stagnation depth will fluctuate over the course of a winter. In addition, the glide constitutive law will depend upon the creep constitutive law used. The next section expands on these points.

4. Discussion of glide constitutive equations as a function of interface and continuum conditions.

Possible alternatives to the assumptions presented in the above description need to be discussed in order to generalize the results:

i. Partly dry interface.

If the interface is only partly wetted, increased drag is to be expected by molecular adhesion of the snow to the surface. The result would be a decrease in glide velocity for a given shear stress or an effective decrease in the stagnation depth over the dry portion.

ii. Interface temperature below the melting point.

If the interface temperature is below 0°C, the snow pack will be frozen to the ground. In this case, the experimental results in the Cascades show that there is no glide when the temperature is below 0°C. The implication is that molecular adhesion is too great to allow glide, i.e., the stagnation depth is zero.

iii. Saturated layer of snow and water layer at the base of the snow pack.

In the case of heavy melt or rain, a water layer may exist at the bottom of the snow pack. Since the permeability of soil may be approximately ten times less than snow, a layer of water may persist. A water layer has the effect of drowning the smallest obstacles to creep. The obstacles higher than the water layer would have to support a greater share of the basal stress resulting in increased glide. The

accompanying saturated layer of snow would, in addition, be subject to a reduction in viscosity due to internal melting, grain lubrication, and pore pressure effects.

The glide data from the spring of 1972 in the Cascades clearly show that the combination of these effects is very important (Figure 3).

iv. Glide crack formation; formation of folds; gliding snow sluffs.

When a water layer is present on a smooth slope, it is possible that virtually all the roughness obstacles are drowned. In this case, the problem becomes unstable, i.e., there is little or no frictional resistance to the whole snow pack sliding off the slope and the stresses in the snow pack are relieved by forming tensile glide cracks in tensile zones. Glide cracks are always associated with times when glide is fast and water is present in the snow pack. This is particularly true after periods of rainfall in the Cascades.

On smooth slopes and for thin snow covers, the glide cracks may be extensive resulting in the release of gliding snow sluffs, particularly at breaks in the terrain. Folds would be expected to form for thin snow covers in compressive zones.

v. Separation of snow from its bed - voids at the base of the snow pack.

It is a matter of experience that when one climbs a timbered or rocky slope, voids are encountered on the downhill side of these obstacles. There is some evidence from snow trenches dug in Montana, U.S.A. (Lang, 1973) that at least for the snow depths and densities found there, cavities are present at the base of the snow pack. Cavities act as stress concentrations which can enhance snow gliding as long as the snow pack is thin enough such that hydrostatic pressure does not close the cavities. If snow is completely in contact with a roughness obstacle, a compressive stress exists on the uphill side of the obstacle and a relatively tensile stress on the downhill side. If the snow is not in contact with the obstacle on the downhill side, the tensile stress on the downhill side is absent. In this case, the longitudinal compressive stress on the uphill side of the obstacle will be doubled and the effective stress concentration will be doubled resulting in faster glide. The analogous problem for glacier sliding has been discussed by Weertman (1964). Creep of snow will tend to further open

the cavities when the hydrostatic pressure is not enough to close them. The mechanism is expected to be most important in early season when the snow pack is thin and creep is relatively fast. No experimental measurements of glide exist in connection with separation of snow from the ground.

vi. Effects of nonlinearity in creep upon the glide constitutive law.

Up to this point, the discussion has been based upon the assumption of a creep mechanism for glide based upon a linear constitutive law. The earlier discussion of creep indicated that the constitutive law for creep deformation is non-linear with the shear viscosity proportional to the bulk stress. In the neutral zone, the viscosity would be very nearly constant at the bottom of the snow pack. However, for tensile or compressive zones this would not be so. Therefore, we generalize the glide constitutive law to:

$$U_o = \frac{D<\tau_{xz}>}{\mu} = \frac{D<\tau_{xz}>}{\frac{K\sigma_{kk}}{2}} \qquad (13)$$

for non-linearity in creep. In this formalism it is assumed that the changes in viscosity due to the changing stress distribution around an obstacle are negligible. This equation is to be regarded as an approximation.

vii. Interdigitation; effects of timber and large obstacles.

It is expected that vegetation intertwined with the snow will introduce increased drag upon the snow pack. To first order it might be assumed that the effect of interdigitation is to introduce a constant drag, τ_o, on the snow pack with a corresponding reduction in glide velocity. This would be equivalent to a reduction in shear stress so that

$$U_o = \frac{D}{\mu}\left(<\tau_{xz}>-\tau_o\right) \qquad (14)$$

to first order. This equation is a form similar to that given by in der Gand and Zupancic (1966).

Timber or large obstacles on a slope would tend to interrupt the creep and glide processes introducing a complicated distribution of shear stress up and down the slope.

viii. Poisson effects; time dependent effects.

The fact that snow is compressible will have an effect upon snow gliding. For a two parameter linear constitutive law, the relationship between the shear stress and glide velocity would still be linear, however.

As the snow densifies and ages with time, the viscosity would be expected to increase with time leading to a slow decrease in glide velocity with time for a constant state of stress. This would be difficult to extract from experimental data because of the fact that the glide velocity is so sensitive to the interface condition and the state of stress is continually changing in the seasonal snow pack. However, this effect might be studied by conducting experiments throughout the snow season in conjunction with glide experiments.

Summary and Discussion

Non-linear constitutive equations are proposed to describe the creep and glide of the snow cover.

The creep constitutive law is not to be regarded as the most general description of the internal deformation of well-settled, well-metamorphosed isothermal snow. The approach taken is that of the simplest explanation consistent with the neutral zone measurements.

A physical and mathematical theory of snow gliding has been presented. In this theory, local creep around bed obstacles is defined as the important mechanism for glide. In the formalism presented, the stagnation depth is defined as the fundamental neutral zone measurement to characterize the topography or terrain roughness. Definition of the stagnation depth suggests a quantitative method of classifying topography of glide slopes as an alternative to the empirical glide factor utilized in the Swiss Guidelines for avalanche defense construction. It is evident that a number of experiments would have to be performed to classify slope topography by stagnation depths. The advantage of such a classification would be that knowledge of the stagnation depth allows immediate formulation of the slip boundary condition from a quantitative physical and mathematical theory.

REFERENCES

Bader, H., and others. 1939. Der Schnee und seine Metamorphose, von H. Bader, R. Haefeli, E. Bucher, J. Neher, O. Eckel, C. Thams, P. Niggli. *Beitrage zur Geologie der Schweiz. Geotechnische Serie. Hydrologie, Lief. 3.* [*English translation: U. S. Snow, Ice and Permafrost Research Establishment. Translation 14, 1954.*]

Brown, C. B., and others. 1973. Incorporation of glide and creep measurements into snow slab mechanics. *Advances in North American Avalanche Technology: 1972 symposium, U. S. Department of Agriculture Forest Service General Technical Report RM-3, p. 7-13.*

Gand, H. R. in der, and Zupancic, M. 1966. Snow gliding and avalanches. *International Union of Geodesy and Geophysics. International Association of Scientific Hydrology. Commission of Snow and Ice, Division of Seasonal Snow Cover and Avalanches. International Symposium on scientific aspects of snow and ice avalanches, 5-10 April 1965, Davos, Switzerland, p. 230-242.*

Kamb, B. 1970. Sliding motion of glaciers: theory and observation. *Reviews of Geophysics and Space Physics, Vol. 8, No. 4, p. 673-728.*

Martinelli, M. 1960. Creep and settlement in an alpine snow-pack. Rocky Mountain Forest and Range Experiment Station, Fort Collins, Colorado, *U. S. Forest Service Research Notes.*

Mellor, M. 1968. Avalanches. *U. S. Cold Regions Research and Engineering Laboratory. Cold regions science and engineering, Hanover, N. H., Part III, Sect. A3d.*

Nye, J. F., 1969. A calculation on the sliding of ice over a wavy surface using a Newtonian viscous approximation. *Proceedings of the Royal Society, Series A, No. 311, p. 445-67.*

Nye, J. F., 1970. Glacier sliding without cavitation in a linear viscous approximation. *Proceeding of the Royal Society, Series A, No. 315, p. 381-403.*

Salm, B., 1967. An attempt to clarify triaxial creep mechanics of snow. (In Oura, H., ed. *Physics of snow and ice: international conference on low temperature science...1966...Proceedings, Vol. I, Pt. 2* [*Sapporo*], *Institute of Low Temperature Science, Hokkaido, University, p. 857-74).*

Sulakvelidze, G. K. 1954. Nekotorye voprosy teploprovoknosti vlazhnogo snega, *Soobscheniia Akad. Nauk Gruzinskoi SSSR, Vol. 15, p. 517-22.*

Weertman, J., 1964. The theory of glacier sliding. *Journal of Glaciology, Vol. 5, No. 39, p. 287-303.*

FIGURE AND TABLE TITLES

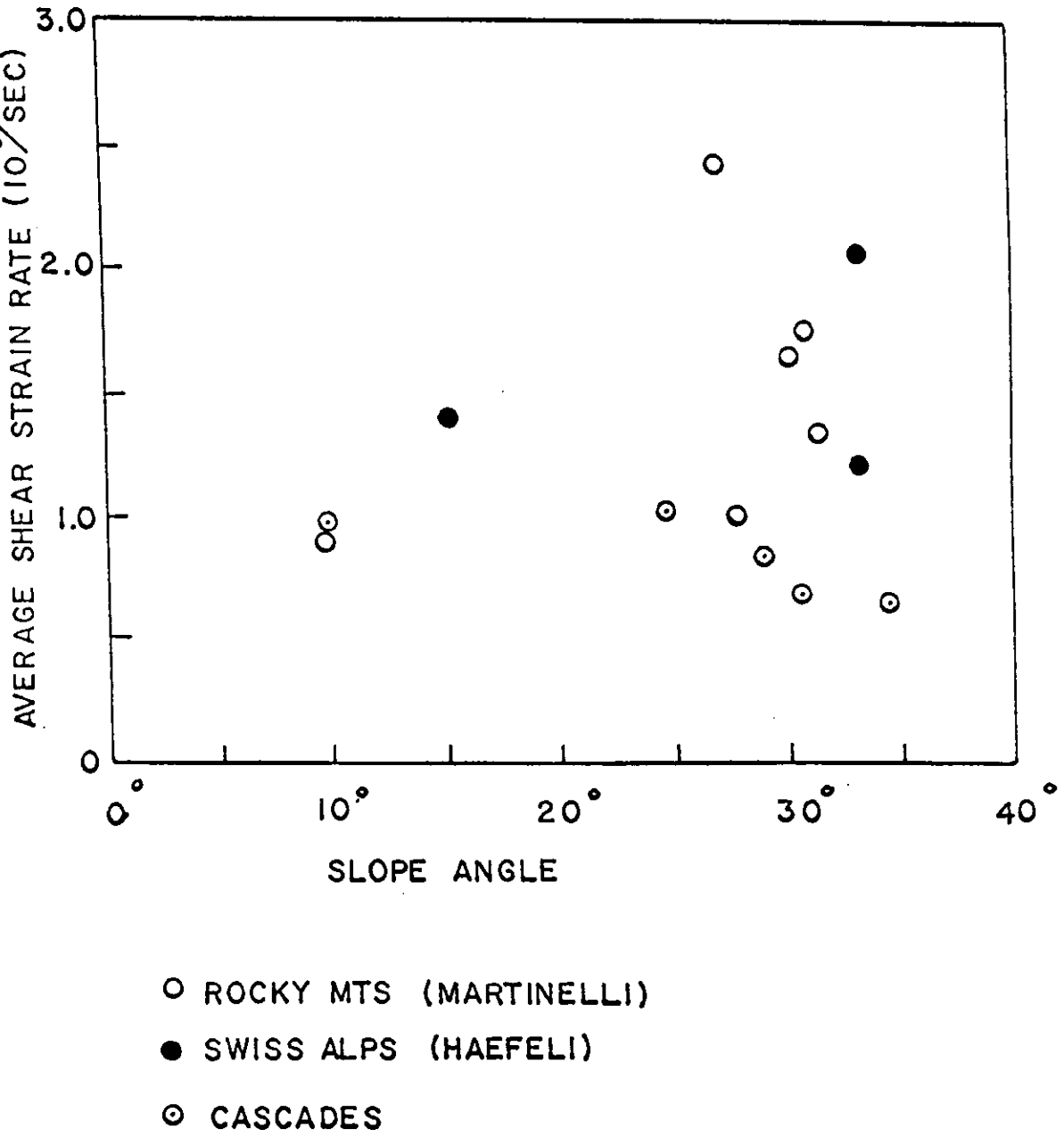
3.0
2.0
1.0
0
AVERAGE SHEAR STRAIN RATE (10^{-8}/SEC)
0°
10°
20°
30°
40°
SLOPE ANGLE
ROCKY MTS (MARTINELLI)
SWISS ALPS (HAEFELI)
CASCADES

FIGURE 1.

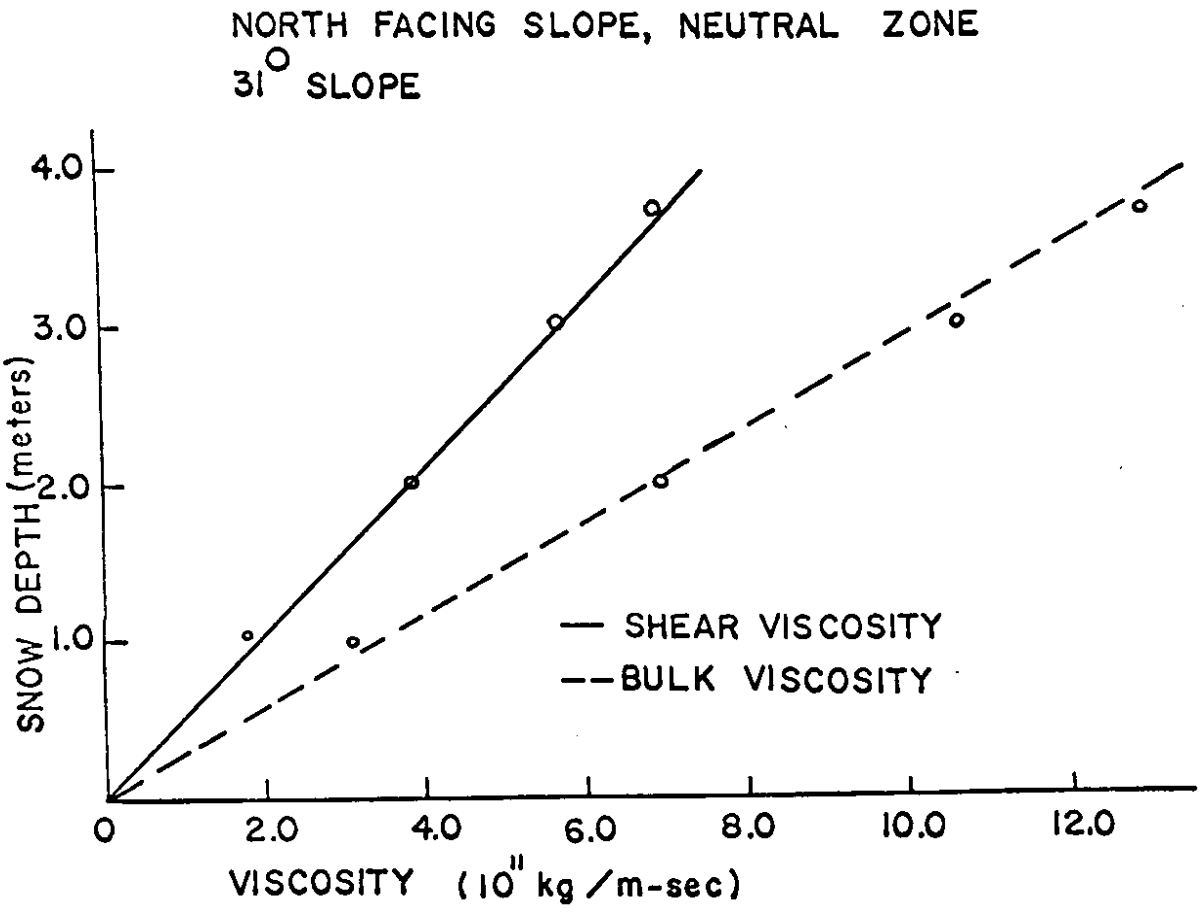
NORTH FACING SLOPE, NEUTRAL ZONE
31° SLOPE
SNOW DEPTH (meters)
4.0
3.0
2.0
1.0
0
2.0
4.0
6.0
8.0
10.0
12.0
VISCOSITY (10^11 kg/m-sec)
— SHEAR VISCOSITY
--BULK VISCOSITY

FIGURE 2.

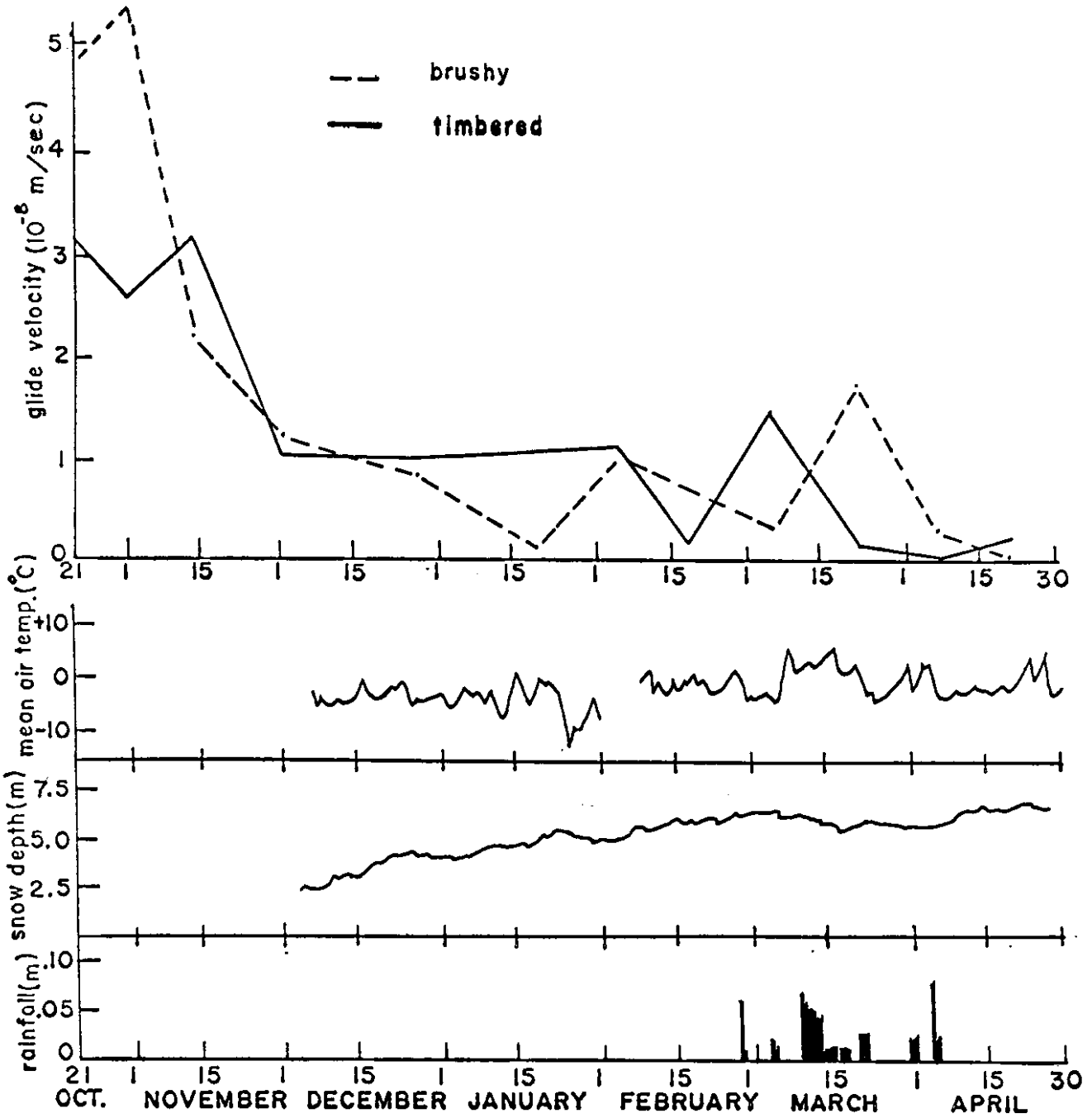
brushy
timbered
glide velocity (10^{-6} m/sec)
mean air temp.(°C)
snow depth(m)
rainfall(m)
OCT.
NOVEMBER
DECEMBER
JANUARY
FEBRUARY
MARCH
APRIL

FIGURE 3.

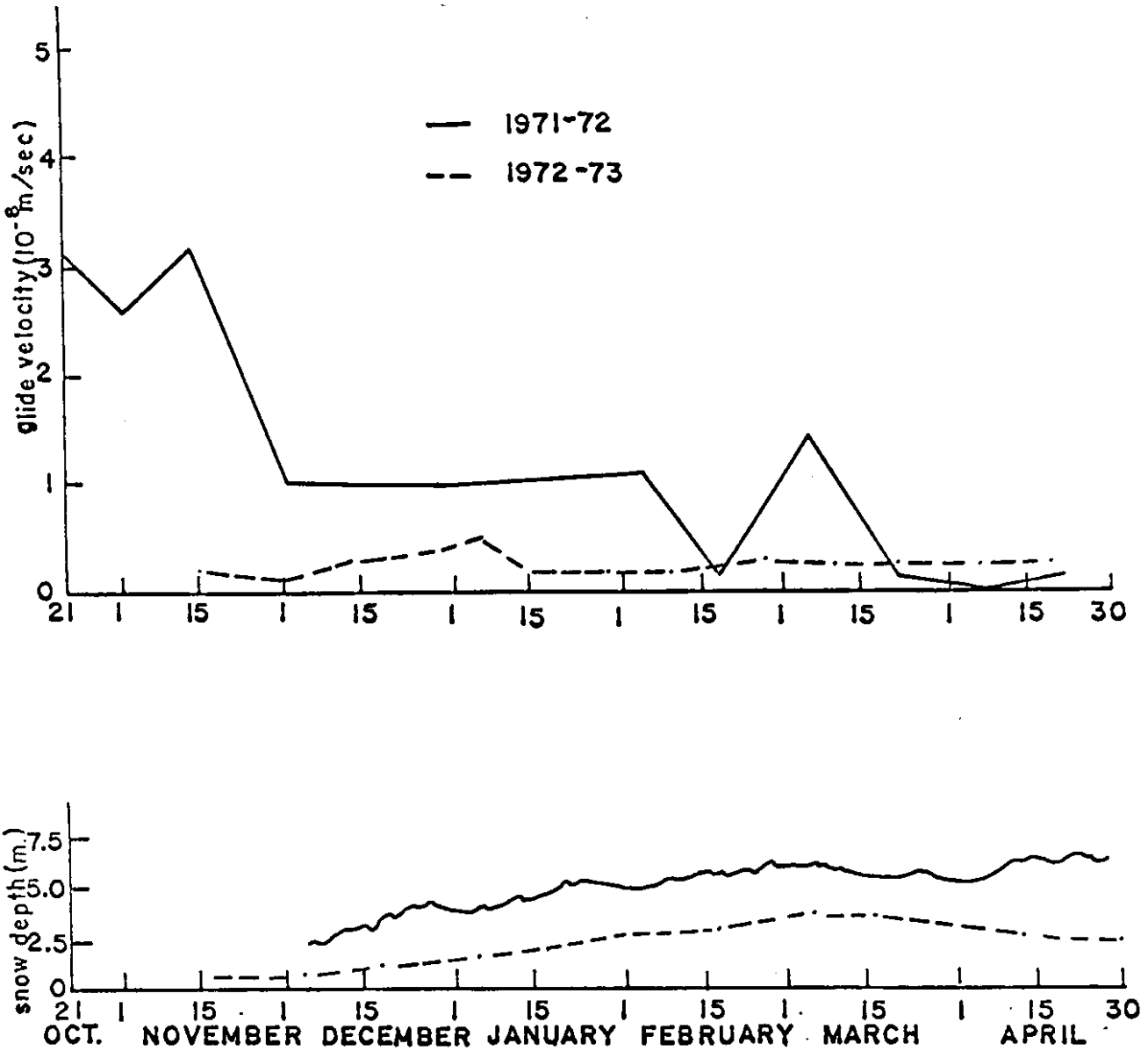
1971-72
1972-73
glide velocity (10⁻⁸m/sec)
snow depth (m.)
OCT.
NOVEMBER
DECEMBER
JANUARY
FEBRUARY
MARCH
APRIL

FIGURE 4.

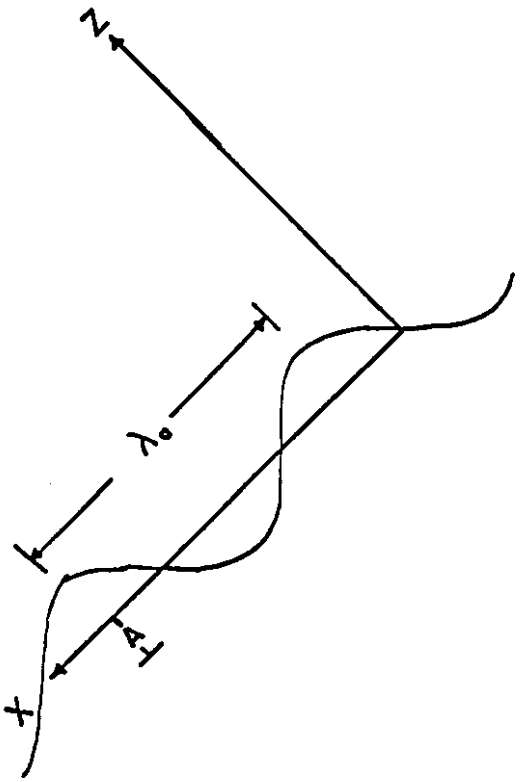

BED GEOMETRY $Z_o = A \cdot SIN(K_o X)$

$$K_o = \frac{2\pi}{\lambda_o}$$

FIGURE 5.

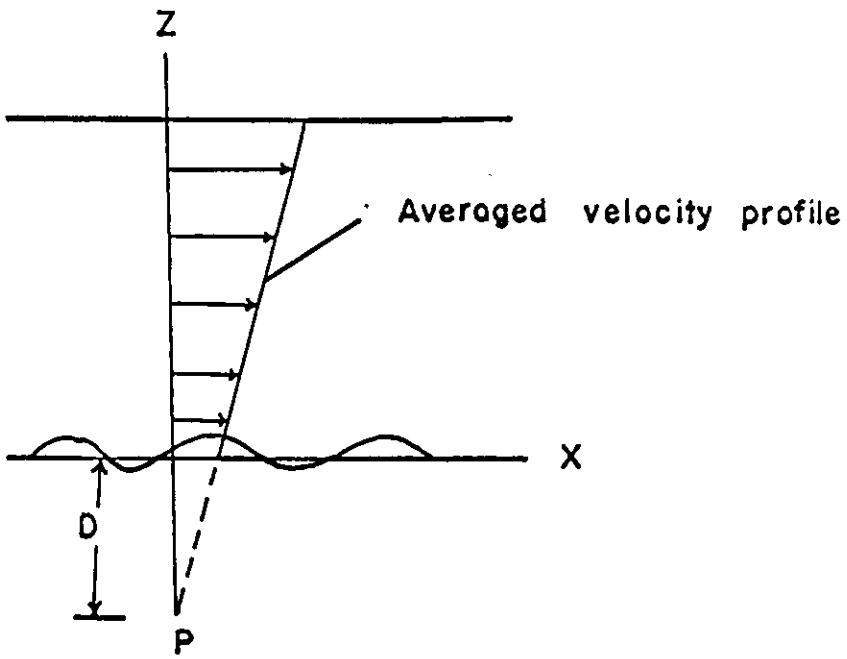

FIGURE 6.

SLOPE ANGLE	AVERAGE DENSITY (KG/M^3)	POISSON RATIO
20°	530	0.31
26°	500	0.32
30°	540	0.23
31°	550	0.27

TABLE I.

STAGNATION DEPTH(m)	SLOPE ANGLE	TERRAIN DESCRIPTION
0.28 (1972) 0.27 (1973)	35°	TIMBERED; SOUTH FACING SLOPE
0.24 (1972) 0.27 (1973)	26°	BRUSHY; SOUTH FACING SLOPE
0.20 (1973)	31°	BRUSHY; NORTH FACING SLOPE
0.33 (1973)	20°	SMOOTH, ROCKY; NORTH FACING SLOPE
0.91 (1973)	40°	GRASSY, SMALL BRUSH; NORTH FACING SLOPE
0.36 (1972)	26°	BRUSHY; WEST FACING SLOPE
0.21 (1972)	31°	TIMBERED; WEST FACING SLOPE

TABLE II.

IN-SITU INVESTIGATIONS OF THE TEMPERATURE DEPENDENCE OF THE CREEP OF LOW DENSITY SNOW

by David M. McClung

Introduction

This report presents preliminary results on the temperature dependence of the creep of low density snow. It is evident from the results obtained thus far that more data are needed to complete this study.

Definition of the temperature dependence in the constitutive equations for snow deformation is an important area for study. Field experience indicates that temperature is an important control on the rate at which dangerous stress situations relax in snow slabs. Qualitatively, dangerous conditions persist longer under colder conditions when the creep rate is lower.

Snow may be considered as an unstable material with respect to creep. At a given test temperature snow will alter its mechanical properties and structure with no given load. Newly fallen snow crystals are inherently thermodynamically unstable entities characterized by high surface free energy. Therefore, creep is not a thermally activated process in the sense that it is normally discussed for materials such as metals.

Another factor which must be dealt with under field conditions that is normally not dealt with in standard engineering creep tests is the effect of temperature gradients on creep. Temperature gradients have the effect of setting up a gradient of saturation vapor pressure causing a second type of metamorphism (recrystallization).

The two types of metamorphism must compete in newly fallen snow. For large temperature gradients the temperature gradient or constructive metamorphism must be dominant. For small temperature gradients the geometric or destructive type of metamorphism must be dominant. There are presumably intermediate cases where the processes compete at similar rates.

Another complication may arise in the case of temperature gradient metamorphism. The possibility of convection in the pores of flow density snow may have to be considered for high enough temperature gradients. It has been estimated that this possibility exists for densities less than $0.3 gm/cm^3$ for high temperature gradients (Yen, 1969).

The indication is, then, that an important parameter is the temperature gradient as well as the temperature. If enough data were available, the hope

would be to formulate equations for each important temperature gradient regime.

Field Measurements

Creep measurements were performed in the Cascades near Mt. Baker and in the San Juan Mountains of Southwestern Colorado. These locations provide approximately the most extreme variations in the winter snow pack for study of creep in the continental United States.

The Mt. Baker area is characterized by relatively small temperature gradients and warm temperatures. Metamorphism would be characterized as destructive metamorphism. The San Juan Mountains are characterized by relatively large temperature gradients, cold temperatures and constructive metamorphism. It is likely that convection plays an important role in the creep process. This has not been shown experimentally, however.

The results in this study were obtained be daily measuring the tilt of poles placed in the snow to various depths. From these measurements it is possible to get the approximate average shear strain rate as a function of time. Temperature measurements were taken with a portable temperature probe.

It should be pointed out that the results thus far are not based on enough data to accurately define the temperature dependence of creep. Accordingly, only gross estimates will be given. The fact that temperature gradients as well as temperatures must be dealt with complicates the problem. Standard creep tests on materials usually deal with isothermal specimens. This is not possible nor desirable under field conditions because temperature gradients must always be dealt with in avalanche research and avalancne snow packs are always subject to temperature gradients except when at the freezing point.

Equation Forms

In general, the steady state creep rate $\dot{\varepsilon}_s$ is related to the test parameters of stress and temperature by an equation of the form:

$$\dot{\varepsilon}_s = f(\sigma,T,st)g(T)$$

where σ is the stress, T is the absolute temperature and st is a structure factor.

The function g(T) normally is represented as

$$g(T) = e^{-Q/RT}$$

where R is the gas constant and Q is termed an activation energy.

Snow creep is not necessarily a thermally activated process in the sense that the above equation is formulated. Destructive metamorphism does not have to be thermally activated in the sense that creep of metals is defined. Therefore, we need not be restricted to the above equation. Mellor (1964, 1974) has pointed out that the function $e^{-Q/RT}$ does not accurately represent the temperature dependence of the creep of snow for temperatures above -5°C. However, it has been shown experimentally that the relation is exponential (Bucher, 1948) and for a given stress and temperature the strain rate is known to increase with temperature.

It is evident that the creep of snow is very complicated and, hence, we begin by using the simplest equation possible to represent the deformation rate. We therefore assume a constant structure factor and a linear relationship between stress and steady state strain rate. Accordingly, the following equation is proposed to describe the creep of snow in order to extend into the high temperature regimes:

$$\mu = \frac{\sigma}{\dot{\epsilon}_s} = K_o e^{-RT/Q}$$

where K_o is constant and μ is the viscosity.

We expect that Q will not in general be a constant in the equation. Q should depend upon the temperature gradient at the very least. Q should, in general, have different values for destructive metamorphism than for constructive metamorphism.

In-Situ Estimates of Strain Rates and Q Values

Figure 1 shows a plot of strain rate as a function of time from measurements on a 23° north facing slope in the Cascades. Figure 2 shows a similar plot from a 34° north facing slope from the San Juan Mountains in Colorado. Steady state creep rates are defined roughly after the creep rate settles down to a slowly decreasing creep rate. For example, the values measured around February 20 for the Colorado results would represent transient values

according to this definition.

The results show that the steady state results are somewhat lower for the Colorado results since the slope was steeper and the densities were somewhat lower on the average. This result may be attributed to the colder temperatures (on the order of 10°C colder at the surface than for the Mt. Baker results). Temperatures for the readings in the Cascades ranged from approximately 0°C to -5°C. Temperatures for the Colorado measurements ranged from -1°C to -19°C.

Results for Q values from both the Cascades and Colorado are of the same order of magnitude. Q values for the measurements in the Cascades show values on the order of 16 cal/mole for temperature gradients on the order of 0.05°C/cm for snow densities on the order of 0.20gm/cm^3. Q values for the Colorado results show values of about 7 cal/mole for temperature gradients on the order of 0.13°C/cm for snow densities on the order of 0.15gm/cm^3.

Discussion

The quoted results are to be taken only as preliminary estimates. Not enough data are available yet to adequately define the temperature dependence in the constitutive equations. The results do seem to indicate that qualitatively creep of snow does slow down at cold temperatures and that snow undergoing constructive metamorphism may have a slightly stronger temperature dependence on the creep rate. The field measurements showed a somewhat larger change in the creep rate for a change in temperature for the temperature gradient metamorphism.

In the formalism presented, the Q value is inversely proportional to the logarithm of the creep rates at different temperatures and it is proportional to the temperature difference. The equation chosen then influenced the results and the Colorado results showed the stronger temperature dependence. According to Bucher's results, we expect that the creep rate will be exponential with the temperature. However, the exact form of the equation is not yet determined. In addition, it is an open question as to whether Bucher's results apply both to snow undergoing destructive metamorphism as well as constructive metamorphism. Much more work is needed on this problem.

References

Mellor, M. "Properties of Snow", Cold Regions Science and Engineering, Part III, Sec. AI. Monograph. U. S. Army Cold Region Res. and Eng. Lab., Hanover, New Hampshire, 1964.

Mellor, M. A Review of Basic Snow Mechanics. Paper presented at International Snow Mechanics Conference, Grindelwald, Switzerland, 1974.

Yen, Yin-Chao. Recent Studies on Snow Properties. In Advances in Hydrosciences, Academic Press, New York, Ven Te Chow, Ed., 1969.

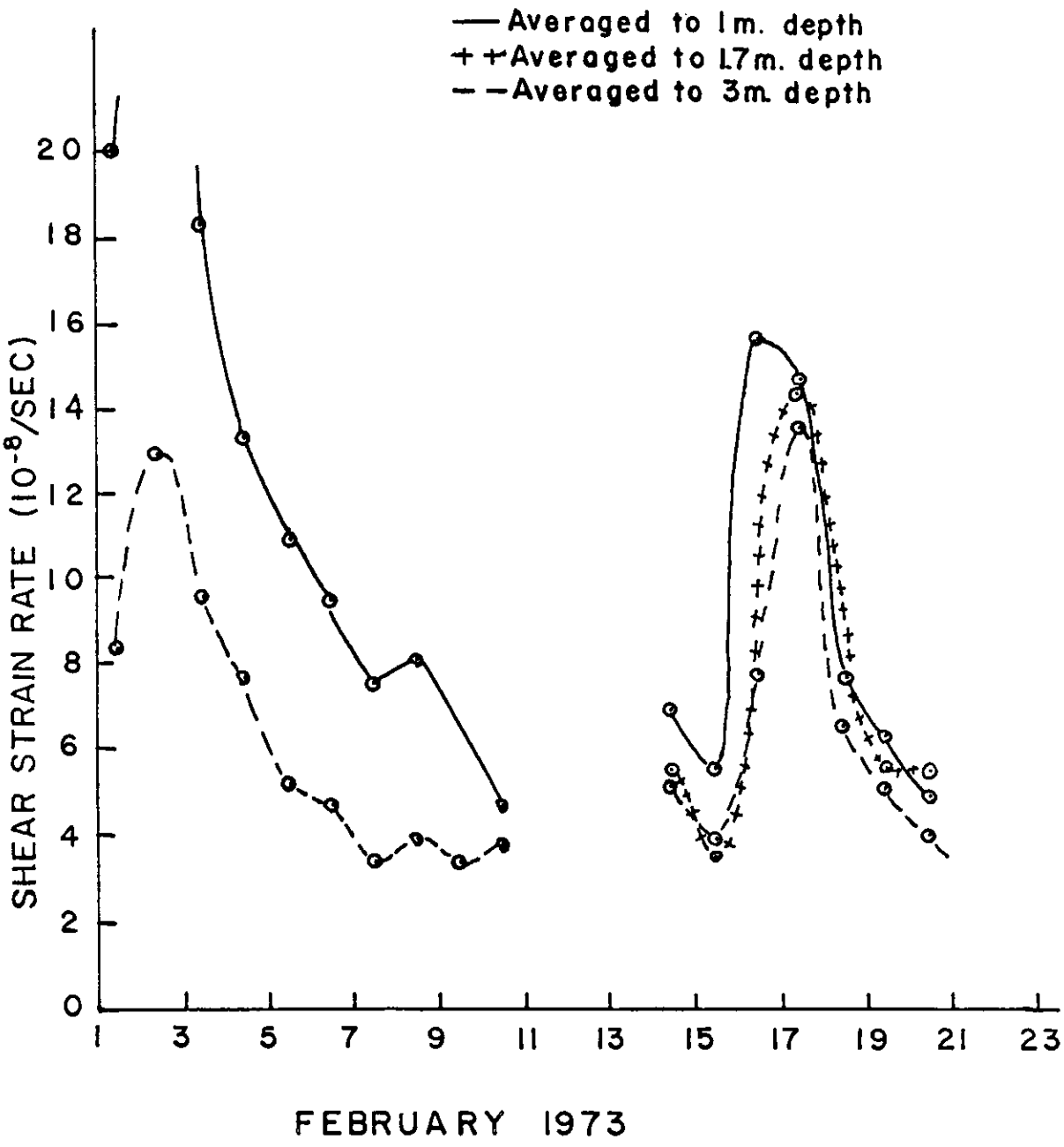
—Averaged to 1m. depth
++Averaged to 1.7m. depth
– –Averaged to 3m. depth
SHEAR STRAIN RATE (10^{-8}/SEC)
0
2
4
6
8
10
12
14
16
18
20
1
3
5
7
9
11
13
15
17
19
21
23
FEBRUARY 1973

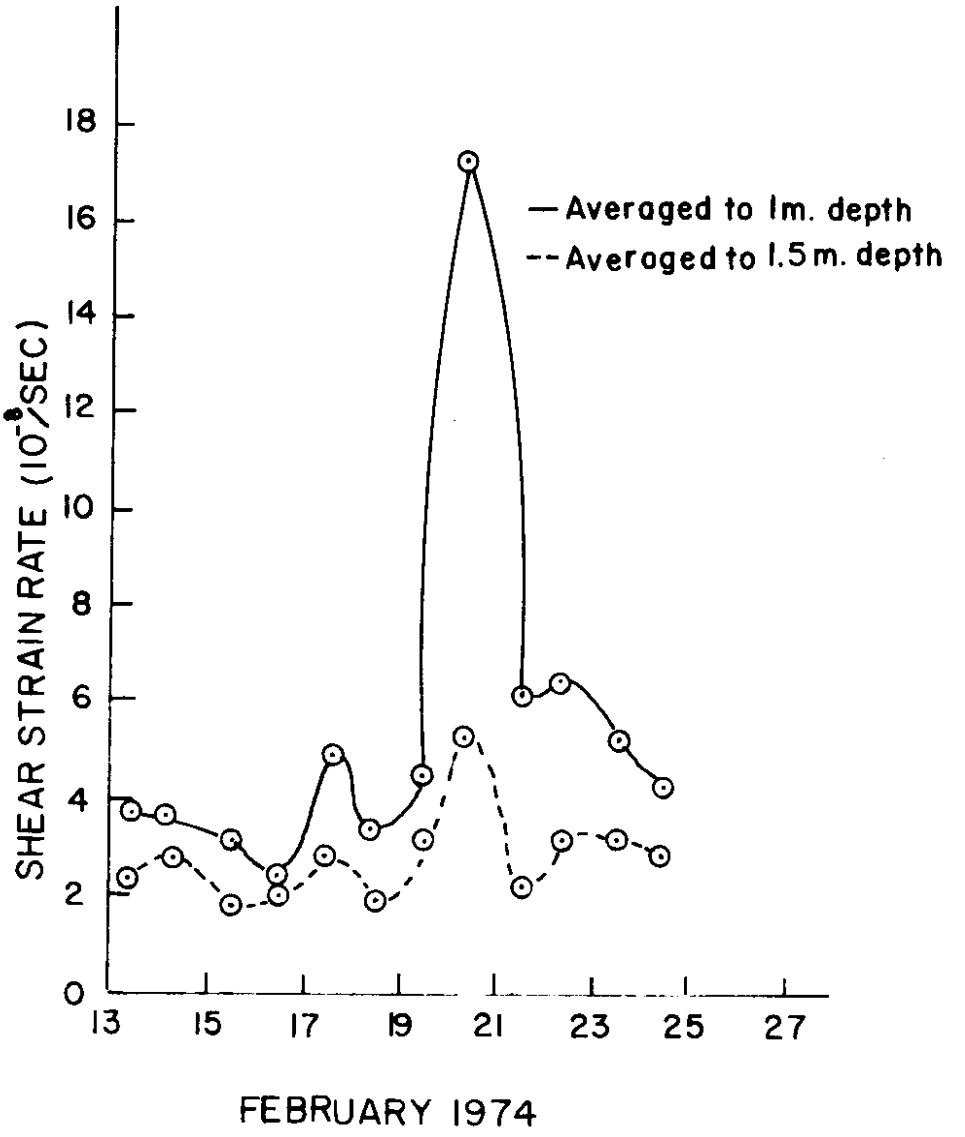
SHEAR STRAIN RATE (10^{-6}/SEC)
0
2
4
6
8
10
12
14
16
18
13
15
17
19
21
23
25
27
FEBRUARY 1974
— Averaged to 1m. depth
-- Averaged to 1.5m. depth

NACHES TUNNEL AVALANCHE RECONNAISSANCE

E. R. LaChapelle

The east and west access routes to the proposed Naches Tunnel under Pyramid Peak appear to offer a route more free of snow avalanche hazard than any of the present Cascade passes.

The west access was investigated by E. R. LaChapelle during a ground reconnaissance on 8/24/72. An aerial reconnaissance of the entire area was made on 7/3/73 by N. Wilson, L. Miller and P. Olson. Wilson made a ground reconnaissance from the west side on 7/14/73 which reached into the upper valley of the North Fork of the Little Naches River and the vicinity of the proposed tunnel east portal.

The various maps furnished by the Department of Highways for this reconnaissance show two different access routes on the west side. The present evaluation is based on the route mapped in the 7/25/60 report from Associated Consultants and the maps accompanying the internal Department memo of 9/9/61 relating to bridge designs. These maps appear to agree on the route and provide the best data for relating the proposed right-of-way to USGS topographic maps. A different west-side access route is shown on the "Aerial Geological Maps" dated August 1961.

West Access Route

The proposed route passes through heavily timbered zones up to and including the tunnel portal. This dense stand of timber, plus the relatively low altitudes reaching only 3600 ft. above sea level at the portal, assures a thoroughly stabilized snow cover. There is no evidence of natural avalanching in this area. Many sidehills are steep enough to generate small snow sluffs which could run among the large trees, or in small open glades, but these would be few at the given altitudes and are unlikely to have any serious effect on the access highway.

Part of the proposed access route passes through Section 30, T. 19 N. R. 11 E. where logging within the Snoqualmie National Forest has recently been in progress. Some of the logged areas are on steep hillsides above the proposed route. There is no present sign of avalanche activity on these logged areas, but it is possible that avalanches of substantial size could fall from them during winters of deep snow. Such avalanches would pose a

threat to the highway. This situation suggests two obvious preventive measures which might be undertaken immediately if there is any reasonable chance that the Naches Tunnel route will be constructed in either the near or distant future. One is to cooperate with the Forest Service to initiate reforestation of those logged slopes above the highway route which could generate avalanches. At this altitude and climate, re-establishment of a stabilizing forest cover ought to be rapid. The other step is to negotiate with the Forest Service to assure that no more potential avalanche slopes will be logged above the proposed highway.

The terrain above about 2500 ft. altitude is steep, especially in the valley of Pyramid Creek. In places, high cutbanks may be a necessary consequence of highway construction. These can introduce local areas for small sluffs and avalanches to develop which can be a nuisance to the highway. The highway design should avoid high cutbanks wherever possible.

Approximately at the west tunnel portal site is a small, open patch of scree on the steep hillside. This could easily be the location for small avalanches in heavy snow winters. The tunnel portal should avoid this scree patch if at all possible. It would also be advisable to maintain an intact forest cover immediately above the portal.

Aerial Reconnaissance

No evidence of avalanche activity was seen in the vicinity of the east portal. The North Fork of the Little Naches River offers an avalanche-free route from the east portal to the junction with Highway 410. Some short, steep slopes and natural cutbanks exist along the river valley which can yield snow sluffs, but these can largely be avoided by prudent choice of the highway location.

East Access Route

There is dense timber cover and no apparent avalanche problems in the vicinity of the proposed east tunnel portal. There is some uncertainty about exactly where the portal is to be located, but the whole area in question is heavily timbered. The optimum site appears to lie north of the river at an altitude of 3600 ft.

Several steep slopes with gradients 35° - 40° lie within Sections 22

and 23, T. 19 N., R. 11 E. on both sides of the North Fork of the Little Naches River. None of these steep slopes show evidence of destructive avalanching, although, as on the west side, they undoubtedly produce sluffs during extreme snow conditions. On the north side of the river within Section 23, slope gradients vary from gentle to flat below the 3600 ft. level. These latter areas are not affected by sluffs from the steep slopes above.

As on the west side, care should be taken to avoid creating high cut banks wherever possible. This is especially true at the tunnel portal.

INVESTIGATION OF SYNOPTIC AND SURFACE WEATHER SITUATIONS LEADING TO MAJOR AVALANCHE CYCLES IN THE WASHINGTON CASCADES FOR THE 1973-74 WINTER

by Mark B. Moore

Summary

An investigation of snow and avalanche activity related to the synoptic and surface weather conditions in the Cascade Mountains of Washington for the period December 1973 to March 1974 has been made. Altogether, nine different avalanche producing storm situations were studied. Snow and weather data from five different Cascade reporting stations (Crystal Mountain, Paradise, Stevens Pass, Alpental and Washington Pass) were correlated with national weather service surface and 500 mb maps for the periods of interest. Figures for new snowfall, total snowfall, and avalanche occurrences serve to characterize the storms. Whenever possible, the general method of avalanche generation is explained for developing weather situations which led to extensive avalanche occurrences at the reporting stations.

In the majority of cases studied, weather situations leading to avalanche release in the Cascades were determined by an upper level low building and moving southeastward from off the coast of southern Alaska over a period of a few days. This situation generally brought a series of surface disturbances through the Cascades, initially aligned north-south and traveling eastward, but gradually shifting to a more southwest to northeast trajectory, as the upper level low moved further southward. Such a shift in alignment and motion of surface fronts resulted in marked effects in avalanche occurrence in the Cascades. Initially, all areas were affected more or less simultaneously by warming, precipitation, and then dropping temperatures as the front passed through (that is, most eastward or northeastward tracking fronts were preceded by a warm sector or ill-defined warm front), but as the upper level flow shifted southwestward, fronts imbedded in this flow affected the southernmost reporting stations first, and in fact, with extreme southward digging of the trough, associated surface lows affected only the southern reporting stations (i.e., Crystal Mountain, Paradise). Thus, in these situations, avalanching may have affected all areas simultaneously at the start of a given avalanche-producing synoptic situation, but a gradual retarding of associated avalanching

at northern stations followed with the southward shifting of the upper level flow into Washington. It should be noted too, that in general a southward-shifting upper level flow into Washington brought substantially more avalanching to the Cascades than a purely zonal flow, other factors being equal (due to increase in the water content of the snow, warming and accompanying increase in the rate of slope loading).

A northwestward flow into Washington at the upper level affected the Cascades quite differently from a southwestward flow. In this situation, the synoptic weather pattern was generally dominated by the juxtaposition of a strong upper level low centered in central Canada and a Pacific high system centered off the northern coast of California. This situation led to surface and upper level disturbances propagating over the top of the Pacific ridge and down the British Columbia coast through Washington. As a result here, the flow was colder and not as moist as a zonal flow and hence led to less major avalanching, but still the geographic progression of avalanching southward through the Cascades was evident. Analagous with extreme cases in the southwestward flow aloft, certain surface fronts only or primarily affected the north Cascades, as at times the surface centers of low pressure passed along the Washington-British Columbia coast and brought only locally heavy snowfall after frontal passage. (It should also be remarked that in all cases, major avalanching was greatly enhanced whenever the upper level jetstream passed directly over the Washington Cascades, as orographic precipitation during these times became especially heavy.)

In all of the above conclusions, variability in type of slides (natural or artificial), time of control, and method of control from area to area must be taken into account. At Stevens Pass, exposure of a major highway to avalanching led to artificial control (by 105 mm recoilless rifle) at all hours of the day, even though natural slides at night and during the day did occur. Compare this type and time of control with Crystal Mountain or Alpental, where control was primarily done in the early morning by ski patrolmen and Forest Service rangers using hand charges (explosives) and 75 mm recoilless rifles. At yet another extreme, compare these situations with Washington Pass or Paradise, where no artificial control work was done, and all slides observed were natural. Such variability limits the conclusions drawn about geographic propagation and timing of avalanching in the Cascades resulting

from any given storm system. This serves to underline the point that avalanching alone cannot be considered as a sufficient indicator of geographic storm progression through the Cascades (or vice versa), especially for storms tracking only slightly off a zonal path. Other geographical factors (e.g., snowfall intensity, winds, etc.) must be and are taken into account for proper storm and avalanche analysis, even given the existence of more standardized control methods and times.

A. Avalanche Activity, December 12-15. Related Synoptic and Surface Weather Summary.

As a result of a relatively strong upper level ridge over the western United States coast from approximately December 8-10, an accompanying period of clear skies and warm day-time temperatures (in the mid-40's during the day at most reporting stations) over most of the Washington Cascades preceded the period of snow and avalanche activity of December 12-15, and, through the generation of a relatively solid melt-freeze crust, produced a fine sliding surface for subsequent snowfall. With the gradual breakdown and eastward movement of the upper level high, a vigorous upper level low dug southeastward from off of the Aleutian chain and intensified, bringing about surface rain along the Washington coast late night on the 10th and early morning of the 11th, and a gradually increasing southwesterly flow aloft. The initial surface front associated with this upper level low and the early coastal precipitation moved quickly across Washington on the 11th, dropping temperatures, and bringing 7-12 inches of snowfall to most of the reporting stations by early morning of the 12th. A second surface cold front approached the coast late morning on the 12th, as both the upper level and surface lows intensified, and, as snowfall records indicate, this now north-south oriented wave passed eastward through the Washington Cascades late afternoon of the 12th and early morning of the 13th, producing continued heavy snowfall at all reporting stations (see accompanying snowfall figures).

Continued southward motion of the upper level disturbance off the Washington coast through the 14th brought increasingly warmer, moister air into Washington by early afternoon of the 14th, with an accompanying increase in temperature and precipitation on the 14th and 15th at all areas. The associated surface warm front, approaching the Washington coast from the southwest in

the early morning of the 15th, was preceded by large amounts of heavy, wet snowfall throughout the Washington Cascades (approximately 10-17 inches of snowfall were reported by 0800 on the 15th at all areas with heavy rain following below 4500-5000 feet). As a result of these weather conditions, moderate direct-action soft-slab avalanche activity was reported at most stations on the 12th, 13th and 14th. Widespread and heavy soft-slab and wet loose avalanching followed at all areas with the onset of wet snow and rain on the 14th and 15th and the accompanying critical slope loading and lubricating effect of the rain.

B. Avalanche Activity, December 25-28. Related Synoptic and Surface Weather Summary.

The meteorological situation for the period December 25-28 was determined primarily by the motion and growth of consecutive large upper level lows digging east-southeastward from the 23rd to the 28th, and their interaction with a building upper level ridge just off the Washington-Oregon coast during this period. On the 23rd of December, the first Aleutian low dominated much of the Washington weather picture, with its circulation bringing in a steady zonal flow to western Washington. Imbedded in this flow, a surface low brought cooling and moderate to heavy snowfall at most Cascade reporting stations on the 22nd, but only moderate avalanching and this only at Alpental on the 23rd. (This minimal observed slide activity was probably due to the stabilizing effect of cooling and surface sloughing of the accumulating dry snow, where the cooling effect had less consequences at Alpental due to its relatively lower elevation.) By the 24th, however, this Aleutian low had moved substantially southward with center now off the central British Columbia coast, and as a result, a more intense surface low associated with this upper disturbance moved southeastward across Washington on the 24th, depositing up to two more feet of snow at some areas. Avalanching associated with this southeasterly propagating disturbance began as noted in the accompanying figures at Washington Pass on the 24th, affecting Alpental and other southern areas by the 26th.

Further southward motion of the first Aleutian low center was substantially halted after the 24th, and in fact, as the upper level high mentioned above moved northward, this dissipating initial Aleutian low slid over the top of

the high eastward to a relatively stationary position over Saskatchewan, and was replaced by the second large Aleutian low. This sequence of events brought a more northwesterly flow into western Washington on the 25th (i.e., as the high pushed northward, airflow aloft into western Washington was forced over the top of the high and then down the British Columbia coast), which gradually shifted zonally by the 28th, as the high subsequently moved much more northward with the Aleutian low flow and became a cutoff center in the Yukon by the 29th (thus allowing for resumption of zonal flow to the south). On a surface flow basis, these upper level developments led to a slight break in weather on the afternoon of the 25th, only to be followed by a vigorous warm sector cold front by late afternoon of the 26th, and the passage of the center of surface low pressure directly thereafter. Winds at most areas, light on the 25th and morning of the 26th and increasing substantially by late afternoon of the 26th, substantiated such surface developments and also created a layer of instability for the heavy, wind-packed snows which followed late on the 26th and on the 27th. (That is, the soft, light snow deposited with little wind at the start of snowfall on the 26th bonded poorly together, and provided an excellent layer of lubrication for the subsequent wind-packed snowfall.) Avalanching during this second system was confined to the southernmost reporting stations, as the center of surface low pressure and the accompanying occluded surface front were confined to and moved across the southern half of the Washington Cascades (see Figure 9 for surface storm development and movement).

C. Avalanche Activity, January 12-15. Related Synoptic and Surface Weather Summary.

The juxtaposition of a very strong Pacific high pressure system and a cold Canadian low dominated the weather for Washington for approximately two weeks prior to the avalanche cycle January 12-15, bringing a cold, dry northerly flow to Washington and therefore, cold, clear weather throughout the period (daytime maximum temperatures remained below 20 degrees at most stations throughout most of the two-week period). This situation provided a somewhat solid sliding surface for subsequent avalanche activity through compaction and a limited melt-freeze cycle, although the colder temperatures inhibited sintering and stabilization of the snowpack except in the topmost

layer (through sun action) and produced pockets of instability (poorly bonded soft snow and sizeable air spaces*) within the snowpack beneath the overlying crust.

Gradually, however, as a strong upper level low dug southward in the northwestern Pacific and another developing low in Canada dug southeastward, the dominating high was slowly dissipated and pushed northward into a cutoff position over Alaska. This development gave rise to a northeasterly traveling occluded surface front imbedded in the developing west-southwesterly flow, which passed through the Cascades on the afternoon and evening of the 12th. This front and the shifting southwesterly flow brought rapidly rising temperatures (and the first snowfall of the month) to all reporting stations in the Cascades, such that by the evening of the 12th, overnight lows at all areas remained in the 30's, and daytime highs on the 13th and 14th approached or surpassed 40°.

By the early afternoon of the 14th, the two developing upper level low pressure systems had joined and this produced an even more southwesterly flow. This fact, combined with the presence of the upper level jet now passing directly over the Washington Cascades, produced heavy orographic precipitation in the Cascades from the 13th through the 15th, almost entirely in the form of rain. (Stevens Pass reported 12+ inches of rain from 1/13-1/16, while Crystal Mountain reported 6.6 inches of rain for a similar period.) Such precipitation was further enhanced by the slow passage of an occluded surface front the day of the 14th and morning of the 15th. This rainfall, following closely behind heavy snowfall on the 12th and 13th, produced major wet loose and slab slide cycles at all areas on the 13th, 14th, and 15th, as bonding of the initial new snowfall to the old sun crust (melt-freeze crust) was minimal. Rain falling after heavy snow percolated through the new snowfall to the crust, and lubricated this surface causing avalanching of the new snowpack.

D. Avalanche Activity, January 22-27. Related Synoptic and Surface Weather Summary.

The weather for the period of avalanche activity January 23-27 was

*Due possibly to the strong temperature gradient and resulting upward vapor diffusion in the snowpack.

determined primarily by the interaction of a large Pacific high (centered at approximately 30° north latitude, 140° longitude, at 0500PST, January 23rd) and a developing low off the coast of southern Alaska. Preceding the period of slide activity, the strong Pacific high brought a cool west-northwesterly flow into the Cascades on the 20th-21st, as the deepening Alaskan low was only beginning to dig southward by the 22nd. However, passage of a weak warm front (associated with the earlier developing low mentioned in the January 12-15 analysis, which brought heavy rainfall to the Cascades and which had been pushed into central Alberta by the above-mentioned developing high) in the late evening of the 21st brought warming and substantial new snowfall to Stevens Pass and Alpental on the 21st and 22nd, followed by heavy avalanching at both areas on the 23rd as indicated in the accompanying avalanche figures. Such avalanche action was primarily due to light snow and cold temperatures at both areas on the 20th and morning of the 21st, followed by heavy wet snow and rapidly rising winds and temperatures late afternoon of the 21st and on the 22nd as the warm front passed through; these conditions created a light, cold, poorly bonding lubricating layer on which the subsequently deposited heavier, wet, wind-packed snow easily slid.

As the upper level low gradually dug southeastward on the 23rd and 24th, the flow aloft shifted southward to a more zonal flow, and a series of short wave disturbances approached the Washington coast. However, the surface high associated with the upper level high remained relatively fixed through the 24th, and cold fronts approaching the coast stalled and became stationary as they were unable to swing into a north-south alignment and move eastward. Thus, a stationary front lingered near the Washington-British Columbia border most of the 24th, while a rapidly dissipating associated warm front (tracking northeastward) passed through southern Washington that same day, bringing substantial snowfall to Paradise, but little elsewhere. Finally, late on the 24th, as the upper level trough began to swing through Washington, the static situation broke down somewhat, and a warm front passed eastward through western Washington late evening on the 24th, followed by a now southeastward moving cold front which brought substantial snow, winds and cooling to all reporting stations by late morning of the 25th. Then as the upper level low dug further southward east of the Cascades, a

second cold front imbedded in the now northwesterly flow aloft brought a final associated warm sector through western Washington the evening of the 26th. The cold front itself, somewhat dissipated, tracked southward through Washington on the afternoon and evening of the 27th. Thus, avalanching on the 26th and 27th occurred as a result of intermittent warm sector, cold sector surface fronts, where warming and accompanying wet snow falling on top of previously deposited colder snow led to extensive natural and artificial snowpack failure (due to both the lubricating effect of the colder underlying snow, and the rapidly increasing loading of the snowpack by the wet snowfall).

Snow Deposition and Surface Weather as Relating to Observed Avalanche Occurrence.

From analysis of the highway department snow and weather observations for the period 1/18 to 1/22, a pattern of snowfall for the slide area at the Stevens Pass ski area may be reconstructed. From the morning of the 18th, when the incoming front signaled the onset of heavy precipitation at Stevens Pass, to the actual time of slide release at 1100 on the 22nd (where now the effects of the warm front were being felt in the air and in the snowpack), a total of 51 centimeters new snowpack was recorded at the top of Stevens Pass, approximately 1000 feet below the starting zone. During this period, approximately 100 centimeters of new snow was added to the existing snowpack in the slide fracture area. Correlating weather observed with stratigraphy found in the snowpack (see Figure 13), it seems probable that the sliding layer was deposited on the evening of the 20th or possibly the early morning of the 21st, when light, dry snow (temperatures were approximately 20°F throughout this period) was falling with only a light wind. Increasing snow intensity and wind throughout the day on the 21st led to heavy deposition of fairly well-compacted snow on top of this light, relatively unstable underlying layer. With increasing temperatures, the night of the 21st and morning of the 22nd, and accompanying heavier, wetter snows, the slope loading became critical, and release of the slide by explosives was inevitable on the 22nd.

E. Avalanche Activity, January 29-February 3. Related Synoptic and Surface Weather Summary.

The weather of the Washington Cascades for the period of interest (1/29 to 2/3) was dominated largely by a low pressure system centered in the upper Northwest Territories at approximately 100° longitude, 70° north latitude at 1700 PST on January 27th. While the center of low pressure remained approximately fixed during the period of interest, the troughs and cutoff lows derived from this system and the associated short waves inherent in the flow were by no means stationary. From analysis of surface and 500 mb weather charts, it is apparent that an upper level trough was digging southeastward from the parent low pressure by 1700 PST on the 27th. This trough subsequently propagated southeastward from the 28th through the 29th, bringing with it an extensive and complicated surface low pressure system which contained an ill-defined southward propagating cold front that passed through western Washington in the late morning and early afternoon of the 29th. See Figures 10 and 11. Extensive avalanching at Washington Pass early on the 29th and at Stevens Pass later in the day on the 29th corroborate this southward motion of the cold front; other more southern areas did not experience heavy avalanching until the 30th.

An extensive surface high pressure system, with centers over Utah and off the central California coast, effectively halted the southeastward progress of this surface low system for a time, such that the center of surface activity (and of convergence) lingered over the Oregon-Washington border south of Yakima for most of the 30th, producing cool temperatures and heavy snowfall throughout the Cascades after frontal passage. However, also during this period the upper level flow gradually shifted from northwesterly on the 28th to southwesterly by the 31st, as a cutoff low formed over central Alaska dug southward. This situation produced warming throughout the Cascades, as imbedded in this new, warmer flow was a warm sector, cold sector frontal system, the warm sector of which passed through the Cascades in a northeasterly direction beginning in the early morning hours of the 31st. This development, accompanied by increased snowfall, led to heavy avalanching at Crystal Mountain and Stevens Pass on the 31st and again on February 1st, as slope loading rapidly became critical, and the following cold front brought continued heavy snowfall through the morning of the 1st. A great deal of instability in the following flow, plus the slow motion of this second surface low pressure center across the northern Cascades, supported moderately heavy snowfall at

Washington and Stevens Passes through the 2nd. This fact, combined with continued avalanche control at Crystal Mountain on the 2nd, led to the secondary avalanche maximum seen in the accompanying combined avalanche occurrence figure.

Snow Deposition and Surface Weather as Relating to Observed Avalanche Occurrence.

From the daily snow and weather observations at Crystal Mountain, a pattern of snow deposition for the period of interest may be found. The 28th as reported at Crystal Mountain was quite warm and a day of intermittent sun, which produced a thin sun crust as noted in the ram resistance plotted in Figure 14. The storm, starting as noted on the afternoon of the 29th, produced rather steady continuous snowfall at Crystal Mountain through the 31st, with 25, 16, and 14 inches of new snowfall reported at the base from 0800 to 0800 of the following day for the 29th, 30th, and 31st, respectively. From correlation of penetrometer, stratigraphy, and wind reports, it appears that the observed sliding layer was produced on the afternoon of the 29th as a result of lessened wind and, therefore, less compaction in a layer approximately 10-20 cm thick. This was followed by heavy snow deposition and strong winds on the evening of the 29th and on through the early morning of the 31st. This heavy snowfall, accompanied by the warming trend on the morning of the 31st, loaded the underlying snowpack to a critical level, favorable for release of medium to large avalanches by explosives and artillery, as observed on the 31st. Thus the sliding layer seems to have been the soft, cohesionless snow falling in the absence of excess winds, but given slightly different weather conditions--i.e., possibly more stability of that cohesionless snow and colder temperatures following directly after formation of the sun crust--the slab shown could very easily have slid off the underlying sun crust.

F. Avalanche Activity, February 19. Related Synoptic and Surface Weather Summary.

The combined effects of a brief period of partial clearing, very light snow and calm winds, followed by a surface cold frontal system which brought initial warming and very heavy snowfall, produced the observed avalanche

cycle on February 19. The 17th as observed at most reporting stations was a day of relatively light winds and some clearing with mild day-time temperatures. This general trend was followed by a rapidly eastward moving warm sector cold front imbedded in a strong zonal flow following passage through Washington of a strong southeastward moving upper level trough on the 17th. The warm sector brought somewhat stronger winds, heavy snowfall and a slight warming on the morning of the 18th, followed by some cooling that afternoon as the cold front swept through. Such a situation, with heavy snowfall at warmer temperatures and stronger winds following the clearing and light snow, inevitably led to the artificially induced avalanching observed on the 19th. Here the quantity and weight of new snow was evidently sufficient to overload the snowpack to the point of artificial release, despite the somewhat stabilizing influence of the warming to cooling trend late on the 18th.

G. Avalanche Activity, February 22. Related Synoptic and Surface Weather Summary.

Snowfall for this avalanche cycle was produced largely by a surface cold front associated with an upper level low off the coast of southern Alaska on the 21st. The sliding surface for this avalanche action resulted primarily from a transitory surface high which yielded clear skies, warm temperatures and a sun crust on the 20th. Wind and snow records at Alpental, Crystal Mountain, and Stevens Pass indicate that the 20th was a calm and relatively clear day with highs in the mid-lower 30's. This situation rapidly deteriorated to increasing wind, cooling temperatures and snow by the morning of the 21st, as the eastward-moving cold front approached the Cascades. See Figure 12. Heavy snow and wind followed through the night of the 21st, with subsequent natural and artificial slab avalanching on the morning of the 22nd. The initial cold snow deposited with light winds did not bond well on the previous day's sun crust, and subsequent heavy wind-packed snowfall caused either extensive instability of the snowpack (which was released by artificial controls) or slope failure (resulting in natural slides).

H. Avalanche Activity, February 26-March 6. Related Synoptic and Surface Weather Summary.

The weather situation leading to the extensive avalanching in the entire Cascades throughout this nine day period was dominated for the most part by a large, vigorous upper level low just west of the central British Columbia coast on February 26, which slowly deepened and progressed eastward through central Canada and the northwest. A series of surface low pressure systems and connected fronts were associated with this upper level long wave trough. The attending southwesterly upper level flow (due to the aforementioned 500 mb trough off the British Columbia coast) brought these disturbances through western Washington almost daily. Late in the day on the 24th and early on the 25th, the first of these short wave disturbances approached and passed through western Washington on an easterly track, bringing strong winds, warming followed by cooling, but only relatively light snowfall by 0800 on the 25th. However, moderate instability in the warm, moist southwesterly flow which followed produced, through fairly intense orographic lifting, increasing snowfall on the 26th and 27th. By late morning on the 28th, a stronger short-wave occluded front passed over the Cascades, once again accompanied by warming and then cooling with heavy snowfall throughout. As a result of such varied temperature changes and increasing snowfall throughout the Cascades during this period, moderately heavy avalanching occurred at most areas from the 26th to the 28th. Here the instability of continuous heavy snowfall at varying temperatures is made evident. Loading of the underlying snowpack occurs most rapidly with heavy snowfall at warm temperatures, and in the above storm situation, this sequence of events occurred both with the orographic precipitation and the second short wave disturbance, thus producing natural and artificial avalanching through critical loading of the underlying colder layers.

On the 1st and the 2nd, the still-persistent southwesterly upper level flow brought another major surface disturbance through the Cascades, as the center of surface low pressure (and, hence, of convergence and maximum precipitation) passed directly over the central Cascades of Washington, bringing especially heavy snowfall to the Snoqualmie Pass area. Alpental reported 12 inches and 21.5 inches, respectively, on the 1st and 2nd. Following this disturbance the upper level flow shifted to almost northerly on the 3rd, as the deepening upper level trough, now pushing as far south as California, moved eastward through Washington. Very strong,more zonal flow in the upper

levels followed the passage of this trough, and the morning of the 4th found another surface disturbance just off the Washington coast. This disturbance, accompanied by strong orographic lifting and the southward shifting of the upper level jetstream to almost directly over north-central Washington, brought again heavy snows to all southern stations on the 4th and 5th. Alpental reported a total of 37 inches of new snowfall during this period, with other southern stations reporting similar amounts in excess of two feet and subsequent heavy avalanching to these stations at this time. Temperatures in Washington also began lowering during this period, as the now deepening upper level low centered in west-central Canada (at approximately 110° latitude, 65° north latitude) gradually dropped 500 mb heights over Washington, pushing colder air southward. This cooling trend became especially noticeable on the 5th, 6th and 7th in the Cascades, as overnight lows (at the 3000-4000 foot level) dropped into the mid-teens on the 5th and 6th, and then to zero on the morning of the 7th. Stevens Pass reported an overnight low of 0°F, and Alpental 4°F the night of the 6th. As a result of the cooling, avalanche activity at most areas dropped off substantially by the 7th, with the exception of Washington Pass, where significant natural releases occurred on the 7th.

Interpretation of Figures

Figures 1-5 include daily snowfall figures and avalanche occurrences for each area indicated. Snowfall figures represent new snowfall for the 24 hour period ending at observation time (0800 at most areas, except Stevens Pass where generally this observation was made at 0530) on the day indicated. For example, 23 inches of snowfall at Paradise on the 27th of December represents that accumulation of new snowfall occurring during the 24 hour period prior to observation (0800) on the morning of the 27th.

Avalanche occurrences indicated are for the day indicated, where non-hashed cross sections imply slab avalanching and hashed sections represent loose avalanching (generally caused by significant warming or rain). No distinction is made here between natural and artificial avalanching, except as noted in the summary; i.e., that all slides observed at Washington Pass and Paradise were natural, while most slides at Alpental, Crystal Mountain, and to a lesser degree Stevens Pass, were artifically induced. Also noted

in the figures are the periods of avalanche activity studied above, listed categorically above the avalanche figures as A, B, ...

The combined avalanche Figure 6 gives the total number of avalanche occurrences for the five reporting stations, with no distinction made between slab and loose avalanching due to some incompleteness of obtainable data, and difficulty in evaluation of avalanche type during adverse weather conditions.

Figure 7 gives total snow depth at all reporting stations, as measured at morning observation time (i.e., 0800 at most stations, 0530 at Stevens Pass). Thus at Paradise, a total of 141 inches total snow depth on January 1 indicates that 141 inches of snow were measured at the observation site at 0800 on the 1st of January.

Figures 9-12 show surface frontal progressions for the given synoptic storm situation and avalanche cycle.

(It should also be noted that in Figure 6, additional storm information is provided with the incorporation of storm plots by the circled numbers above avalanche occurrences. The storm plots were recorded and provided by avalanche observer Frank Almquist at Washington Pass and are given in Figure 8.)

FIGURE 1

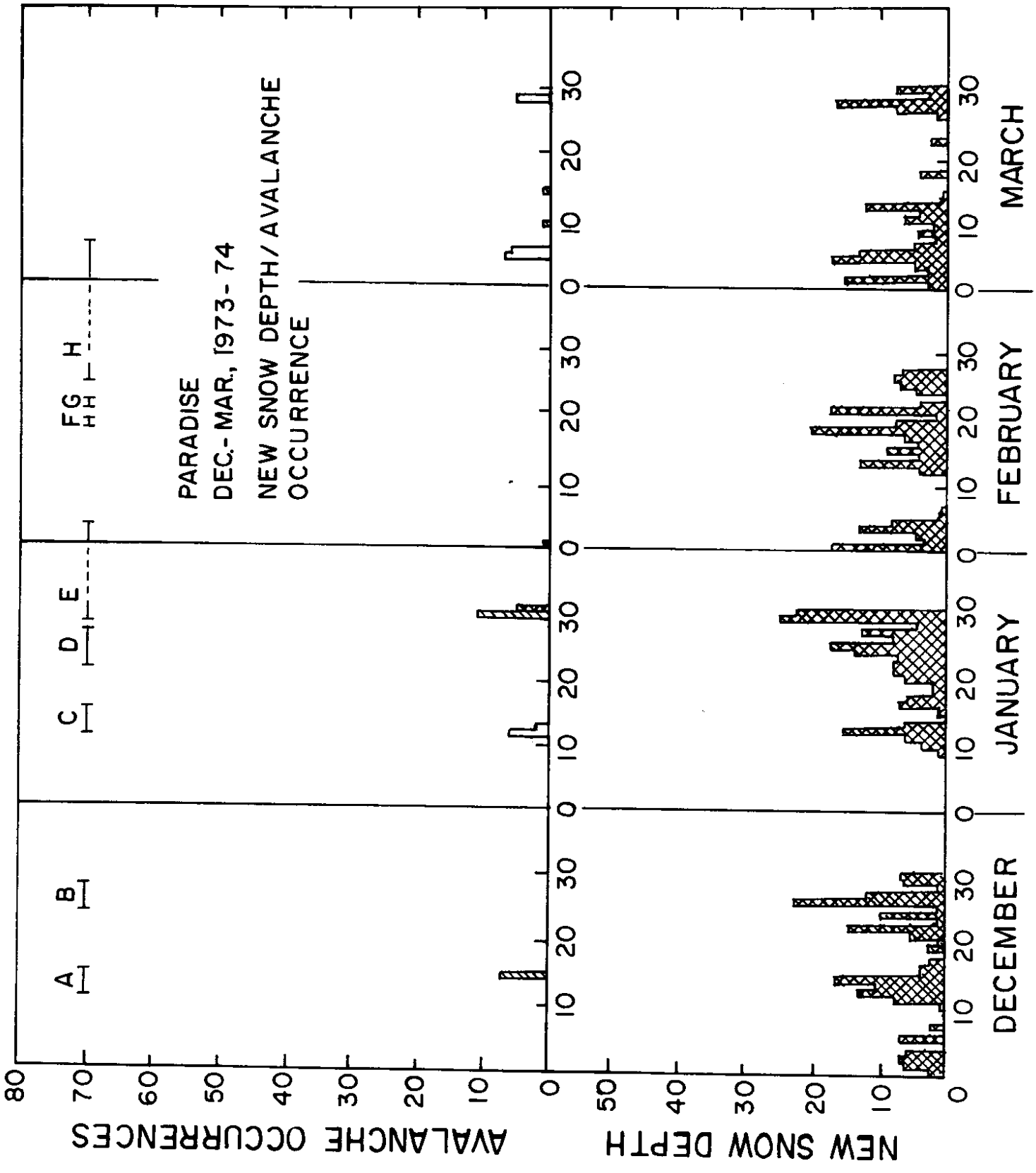
PARADISE
DEC.- MAR., 1973- 74
NEW SNOW DEPTH / AVALANCHE OCCURRENCE
A
B
C
D
E
F
G
H
AVALANCHE OCCURRENCES
NEW SNOW DEPTH
DECEMBER
JANUARY
FEBRUARY
MARCH

FIGURE 2

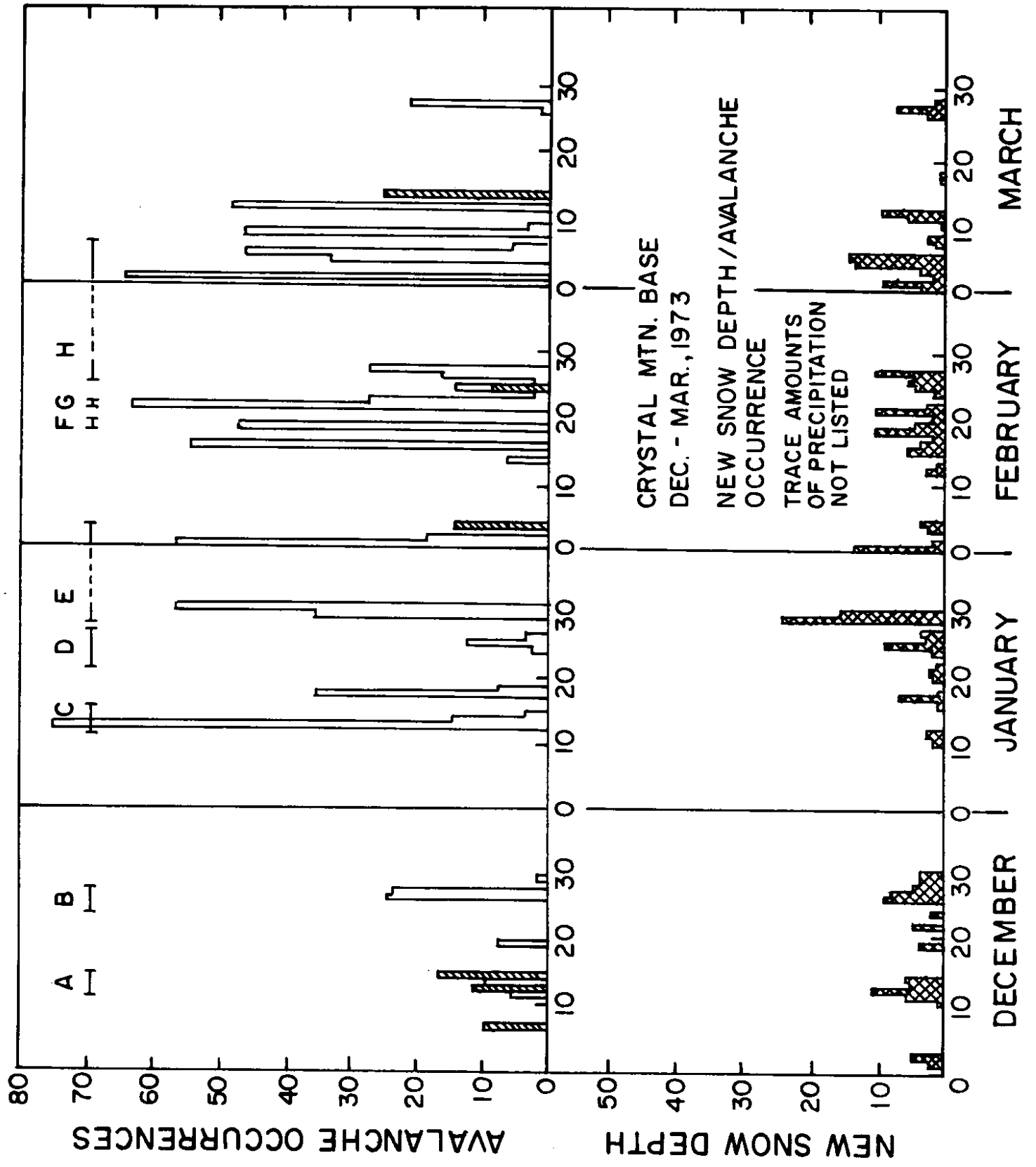
AVALANCHE OCCURRENCES
NEW SNOW DEPTH
A
B
C
D
E
F G H
CRYSTAL MTN. BASE
DEC. - MAR., 1973
NEW SNOW DEPTH / AVALANCHE OCCURRENCE
TRACE AMOUNTS OF PRECIPITATION NOT LISTED
DECEMBER
JANUARY
FEBRUARY
MARCH

FIGURE 3

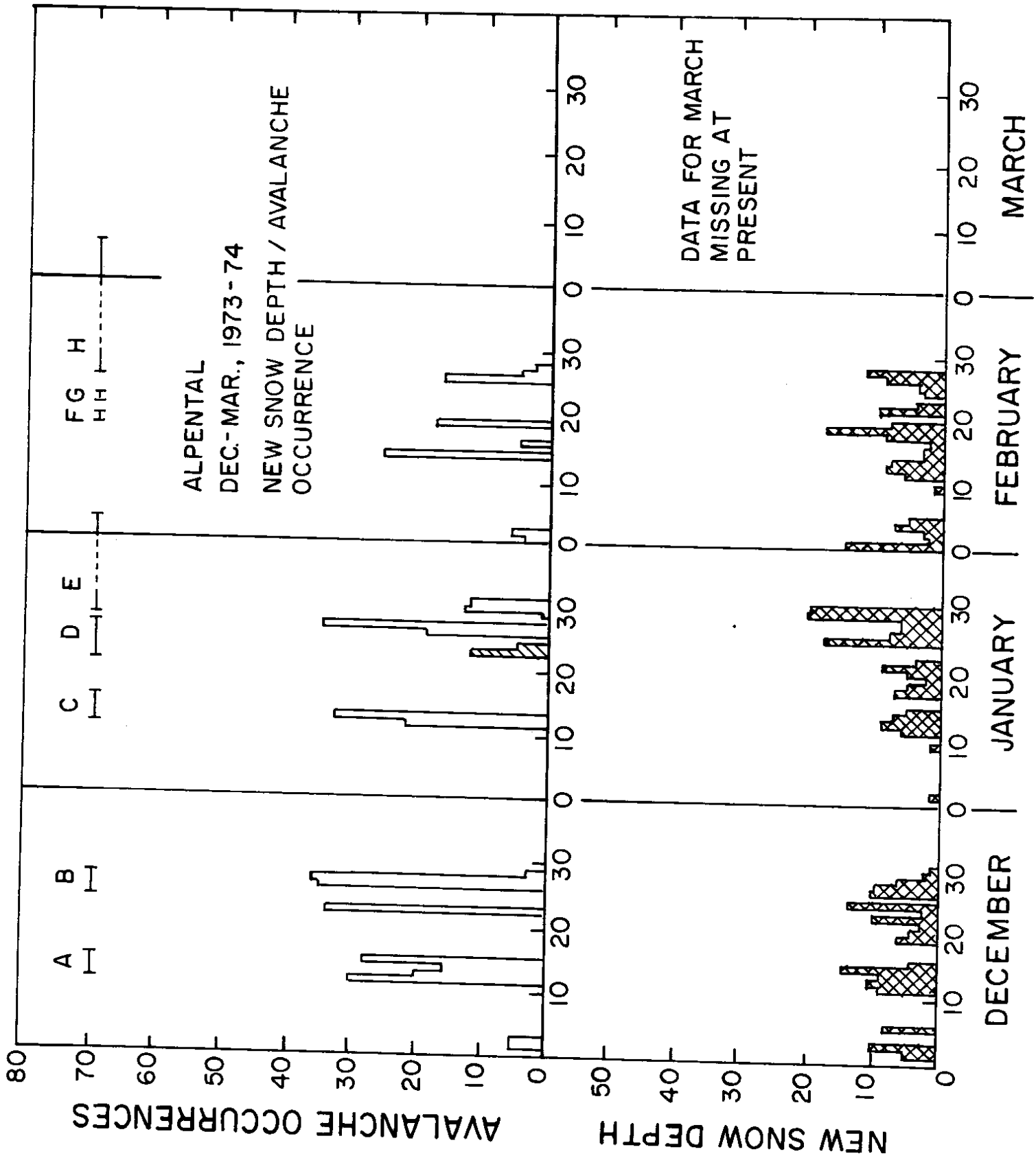
ALPENTAL
DEC.-MAR., 1973-74
NEW SNOW DEPTH / AVALANCHE OCCURRENCE
DATA FOR MARCH MISSING AT PRESENT
A
B
C
D
E
F
G
H
AVALANCHE OCCURRENCES
NEW SNOW DEPTH
DECEMBER
JANUARY
FEBRUARY
MARCH

FIGURE 4

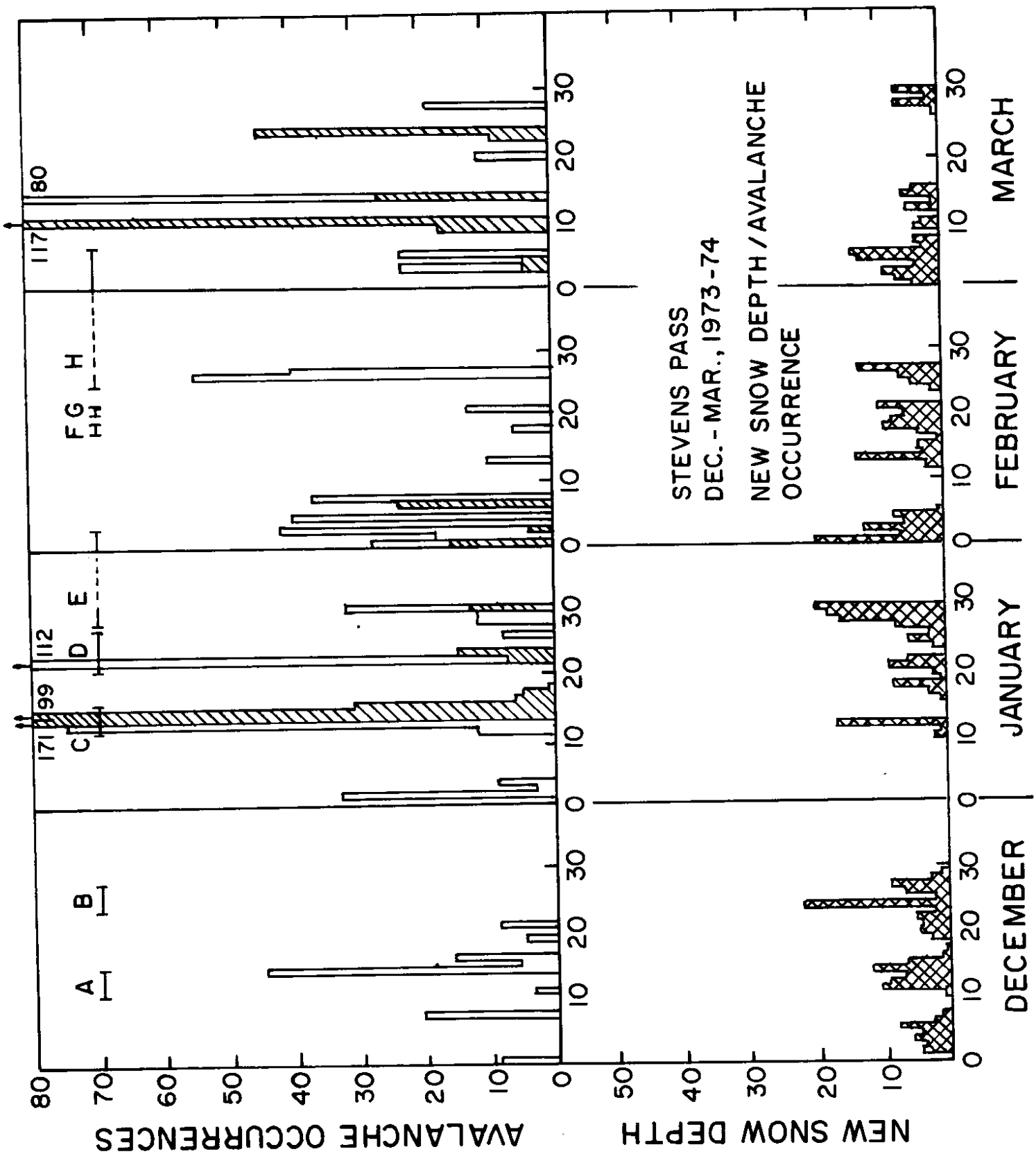
AVALANCHE OCCURRENCES
NEW SNOW DEPTH
STEVENS PASS
DEC.-MAR., 1973-74
NEW SNOW DEPTH / AVALANCHE OCCURRENCE
DECEMBER
JANUARY
FEBRUARY
MARCH
A
B
C
D
E
F
G
H
171
99
112
117
80

FIGURE 5

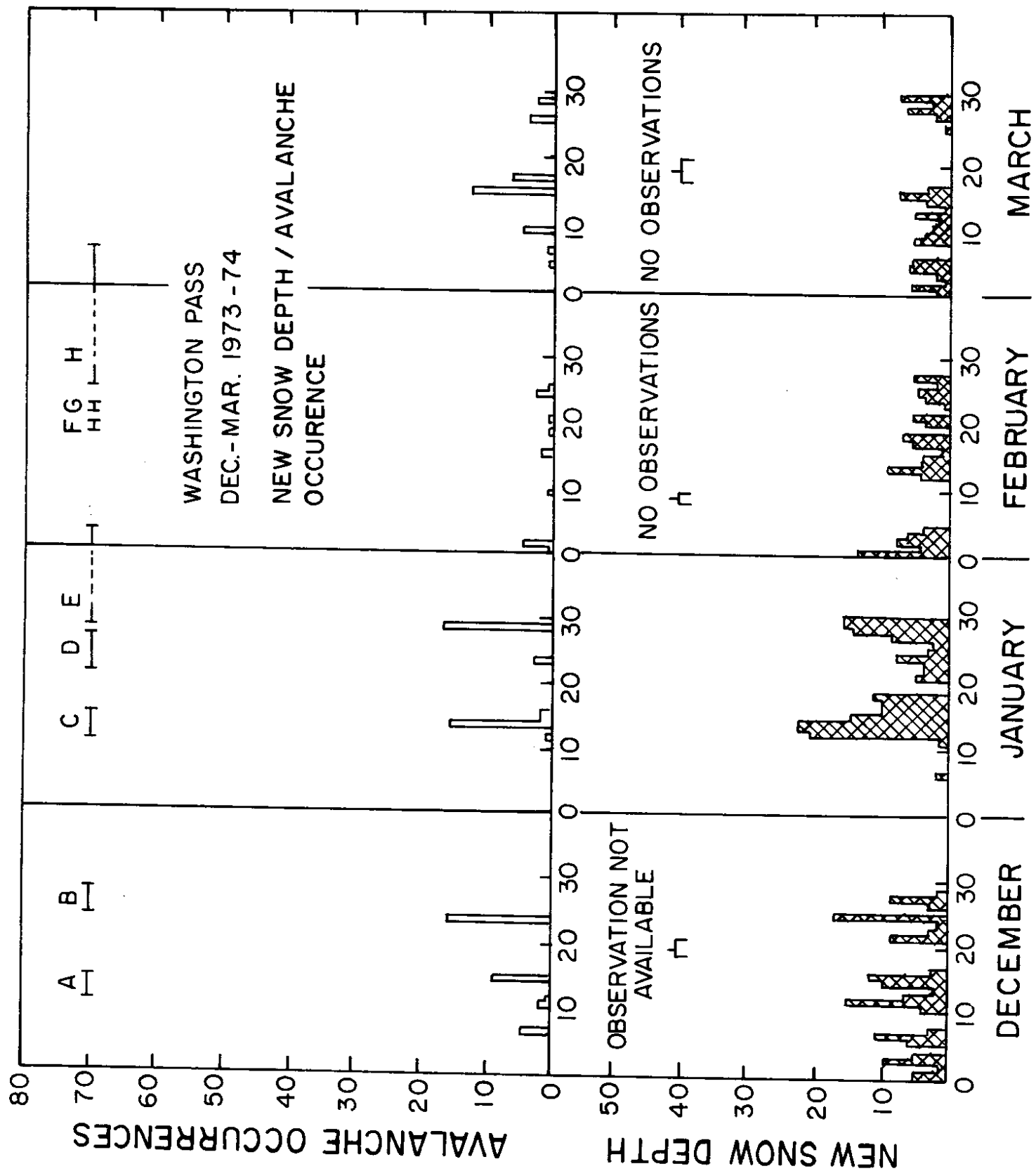
WASHINGTON PASS
DEC.-MAR. 1973-74
NEW SNOW DEPTH / AVALANCHE OCCURENCE
AVALANCHE OCCURRENCES
NEW SNOW DEPTH
A
B
C
D
E
F
G
H
OBSERVATION NOT AVAILABLE
NO OBSERVATIONS
NO OBSERVATIONS
DECEMBER
JANUARY
FEBRUARY
MARCH

FIGURE 6

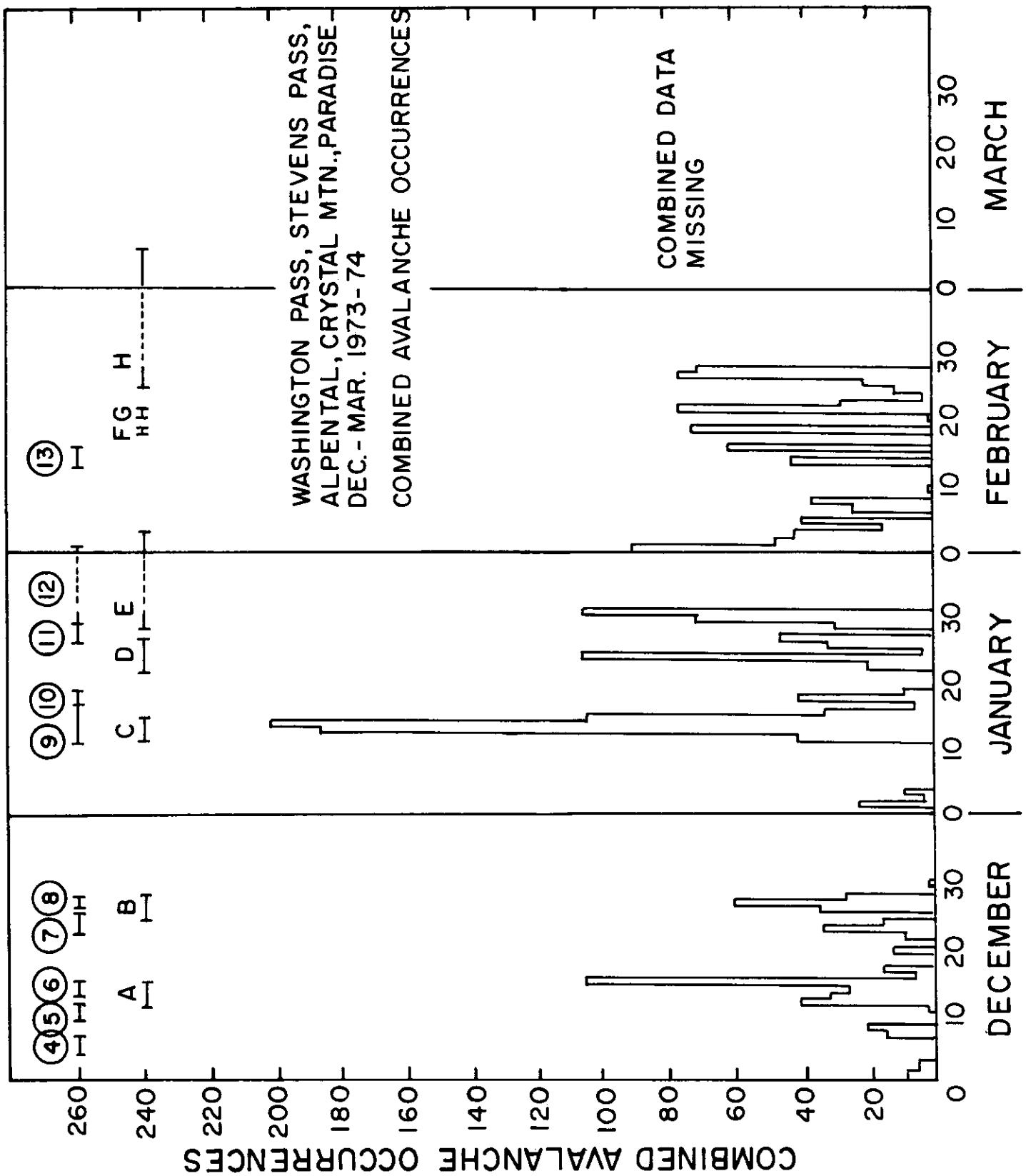
WASHINGTON PASS, STEVENS PASS,
ALPENTAL, CRYSTAL MTN., PARADISE
DEC. - MAR. 1973-74
COMBINED AVALANCHE OCCURRENCES
COMBINED DATA
MISSING
COMBINED AVALANCHE OCCURRENCES
DECEMBER
JANUARY
FEBRUARY
MARCH
A
B
C
D
E
F
G
H
4
5
6
7
8
9
10
11
12
13

FIGURE 7

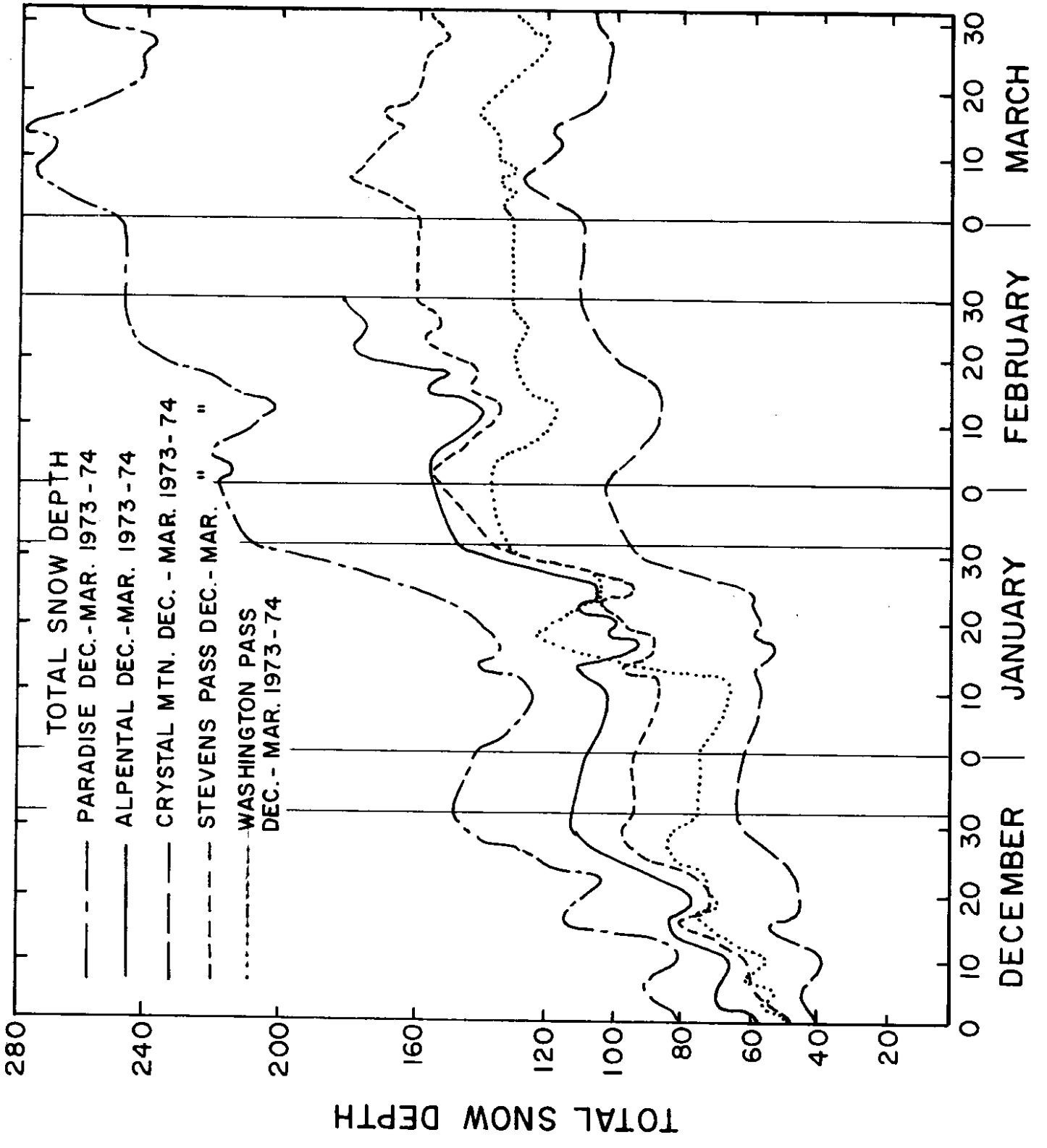
TOTAL SNOW DEPTH
PARADISE DEC.-MAR. 1973-74
ALPENTAL DEC.-MAR. 1973-74
CRYSTAL MTN. DEC.-MAR. 1973-74
STEVENS PASS DEC.-MAR. "
WASHINGTON PASS DEC.-MAR. 1973-74
TOTAL SNOW DEPTH
280
240
200
160
120
100
80
60
40
20
0
10
20
30
DECEMBER
JANUARY
FEBRUARY
MARCH

FIGURE 8

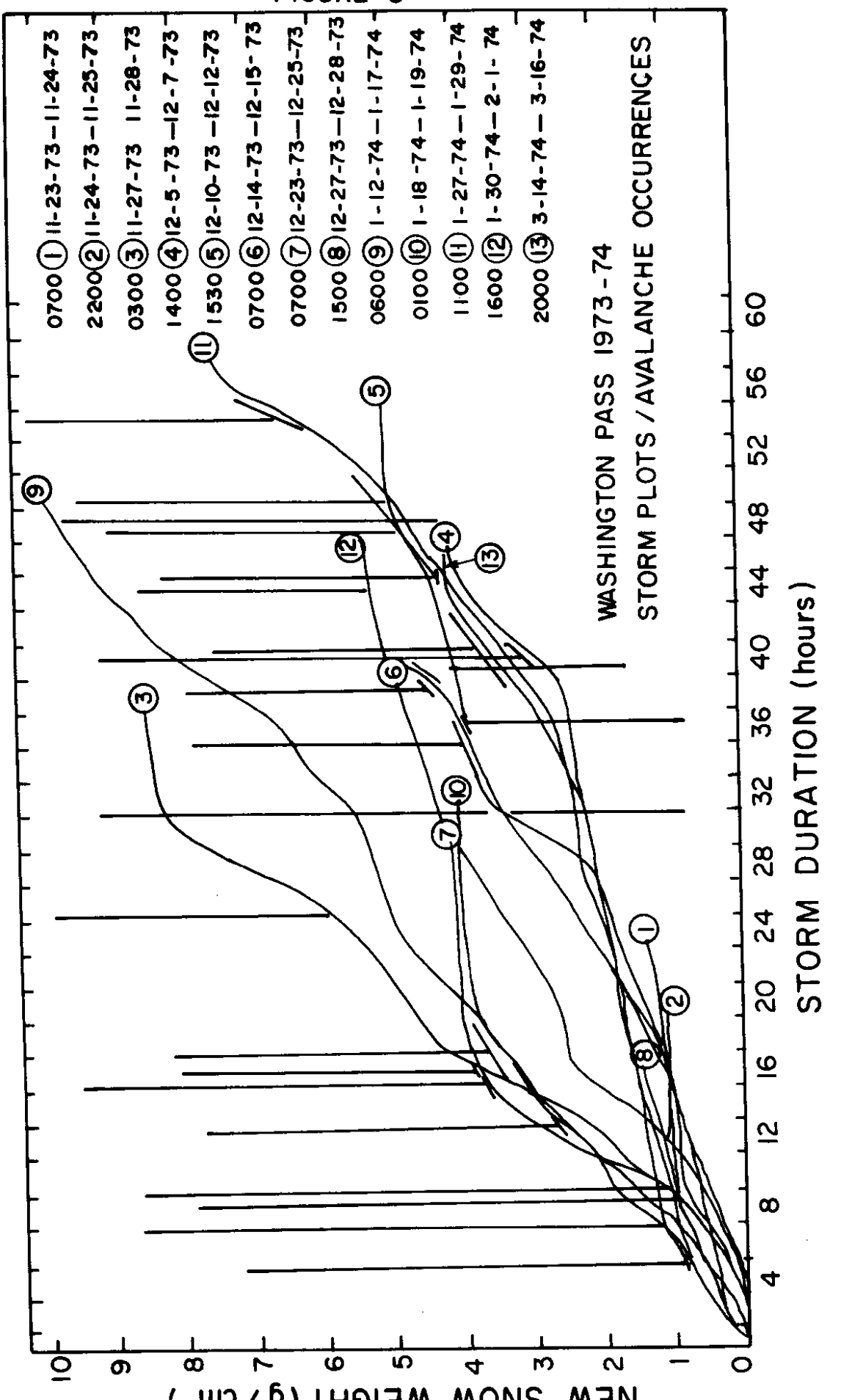
WASHINGTON PASS 1973-74
STORM PLOTS / AVALANCHE OCCURRENCES
0700 ① 11-23-73 — 11-24-73
2200 ② 11-24-73 — 11-25-73
0300 ③ 11-27-73 11-28-73
1400 ④ 12-5-73 — 12-7-73
1530 ⑤ 12-10-73 — 12-12-73
0700 ⑥ 12-14-73 — 12-15-73
0700 ⑦ 12-23-73 — 12-25-73
1500 ⑧ 12-27-73 — 12-28-73
0600 ⑨ 1-12-74 — 1-17-74
0100 ⑩ 1-18-74 — 1-19-74
1100 ⑪ 1-27-74 — 1-29-74
1600 ⑫ 1-30-74 — 2-1-74
2000 ⑬ 3-14-74 — 3-16-74
NEW SNOW WEIGHT (g / cm²)
STORM DURATION (hours)
0 1 2 3 4 5 6 7 8 9 10
4 8 12 16 20 24 28 32 36 40 44 48 52 56 60

FIGURE 9

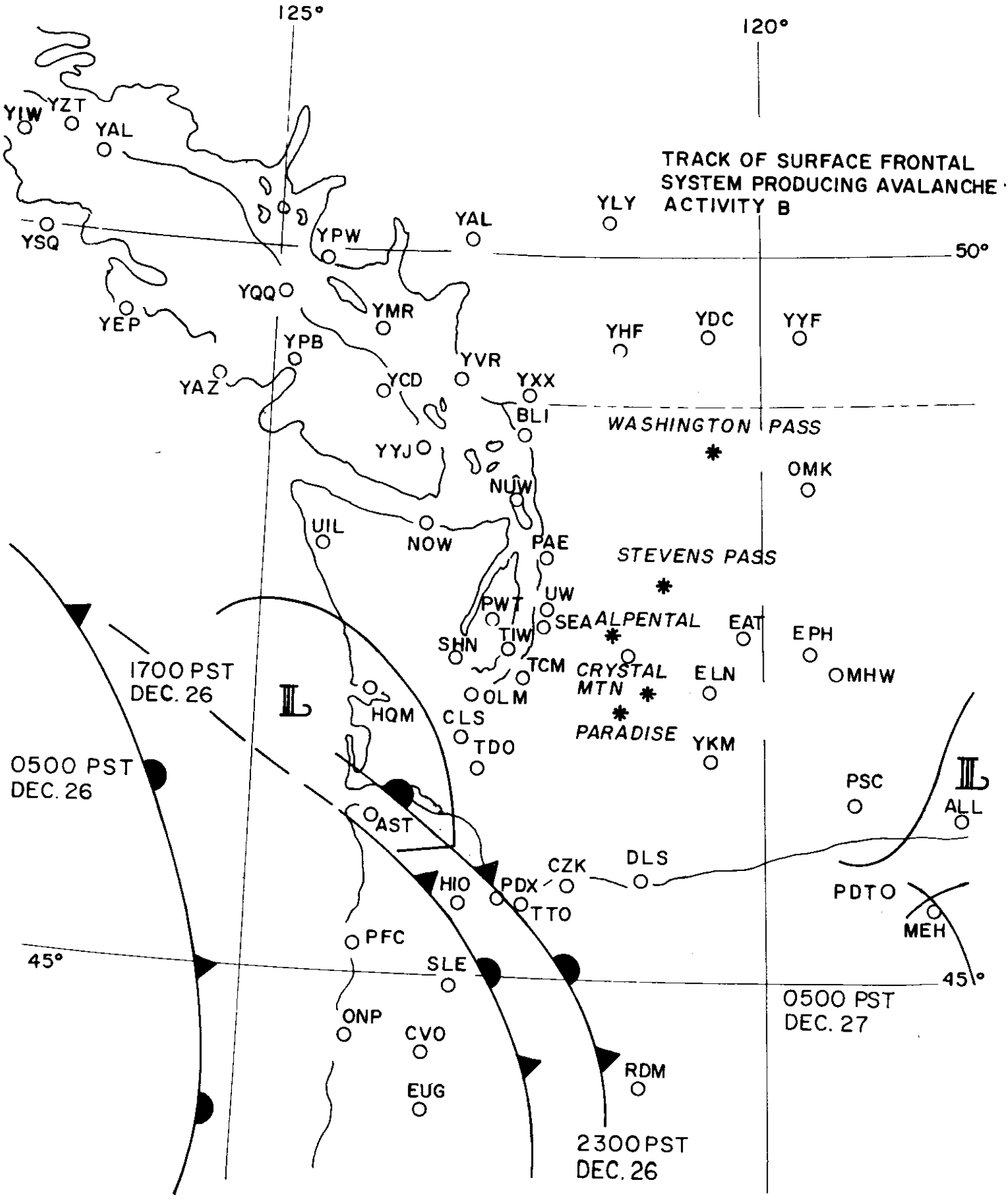
125°
120°
TRACK OF SURFACE FRONTAL SYSTEM PRODUCING AVALANCHE ACTIVITY B
YIW
YZT
YAL
YSQ
YPW
YAL
YLY
50°
YQQ
YMR
YEP
YPB
YHF
YDC
YYF
YAZ
YCD
YVR
YXX
BLI
WASHINGTON PASS
YYJ
OMK
NUW
UIL
NOW
PAE
STEVENS PASS
UW
PWT
SEA
ALPENTAL
EAT
EPH
SHN
TIW
TCM
CRYSTAL MTN
ELN
OMHW
1700 PST DEC. 26
OLM
HQM
CLS
PARADISE
YKM
TDO
0500 PST DEC. 26
PSC
ALL
AST
CZK
DLS
HIO
PDX
PDTO
TTO
MEH
PFC
45°
SLE
45°
0500 PST DEC. 27
ONP
CVO
RDM
EUG
2300 PST DEC. 26

FIGURE 10

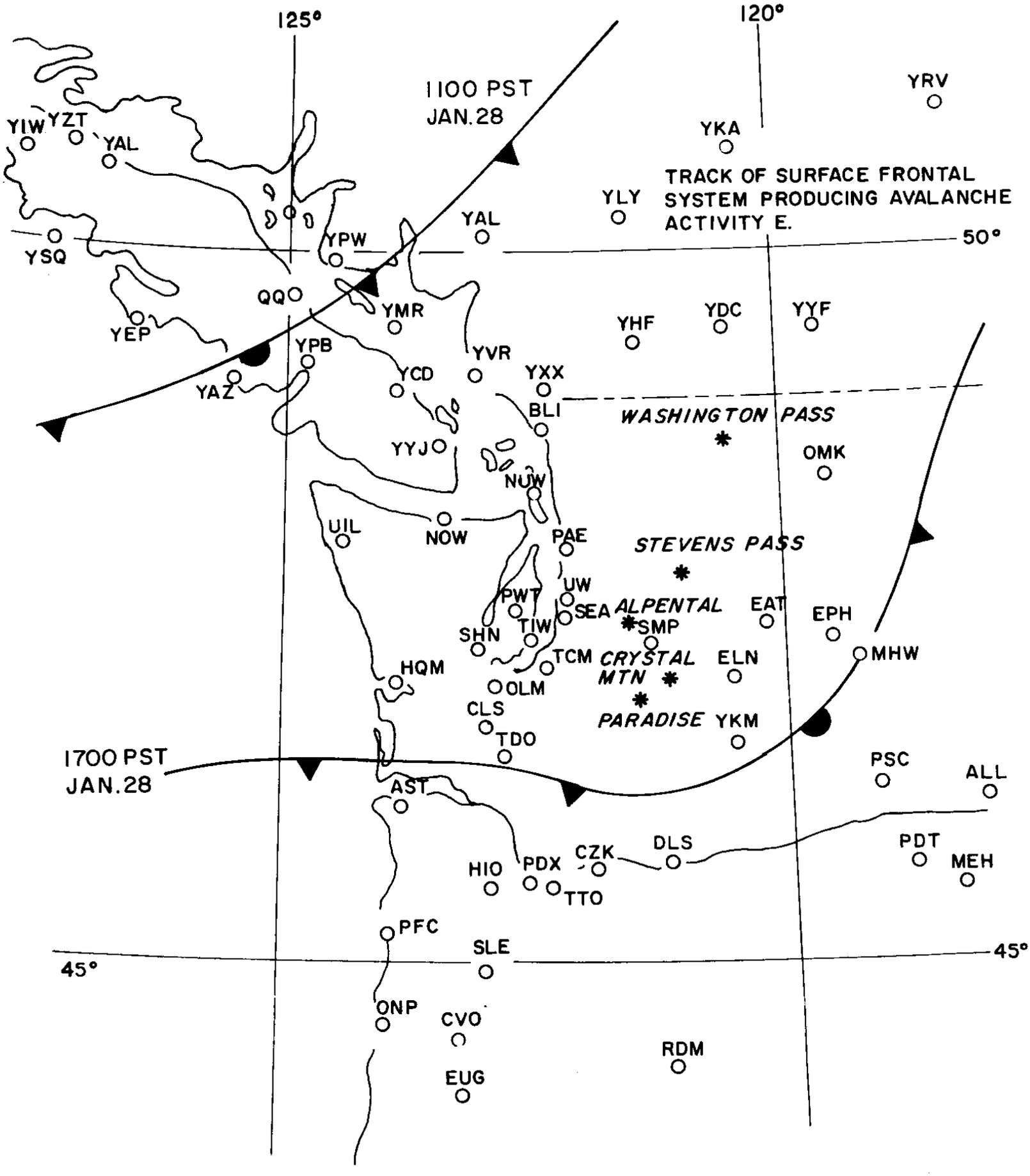
125°
120°
1100 PST
JAN. 28
TRACK OF SURFACE FRONTAL SYSTEM PRODUCING AVALANCHE ACTIVITY E.
YIW
YZT
YAL
YSQ
YPW
YAL
YLY
YKA
YRV
50°
QQ
YMR
YEP
YPB
YAZ
YCD
YVR
YXX
YHF
YDC
YYF
BLI
WASHINGTON PASS
YYJ
OMK
NUW
UIL
NOW
PAE
STEVENS PASS
UW
PWT
SEA
ALPENTAL
EAT
EPH
SHN
TIW
SMP
TCM
CRYSTAL MTN
ELN
MHW
HQM
OLM
CLS
PARADISE
YKM
TDO
1700 PST
JAN. 28
PSC
ALL
AST
DLS
CZK
PDT
HIO
PDX
MEH
TTO
PFC
SLE
45°
45°
ONP
CVO
RDM
EUG

FIGURE 11

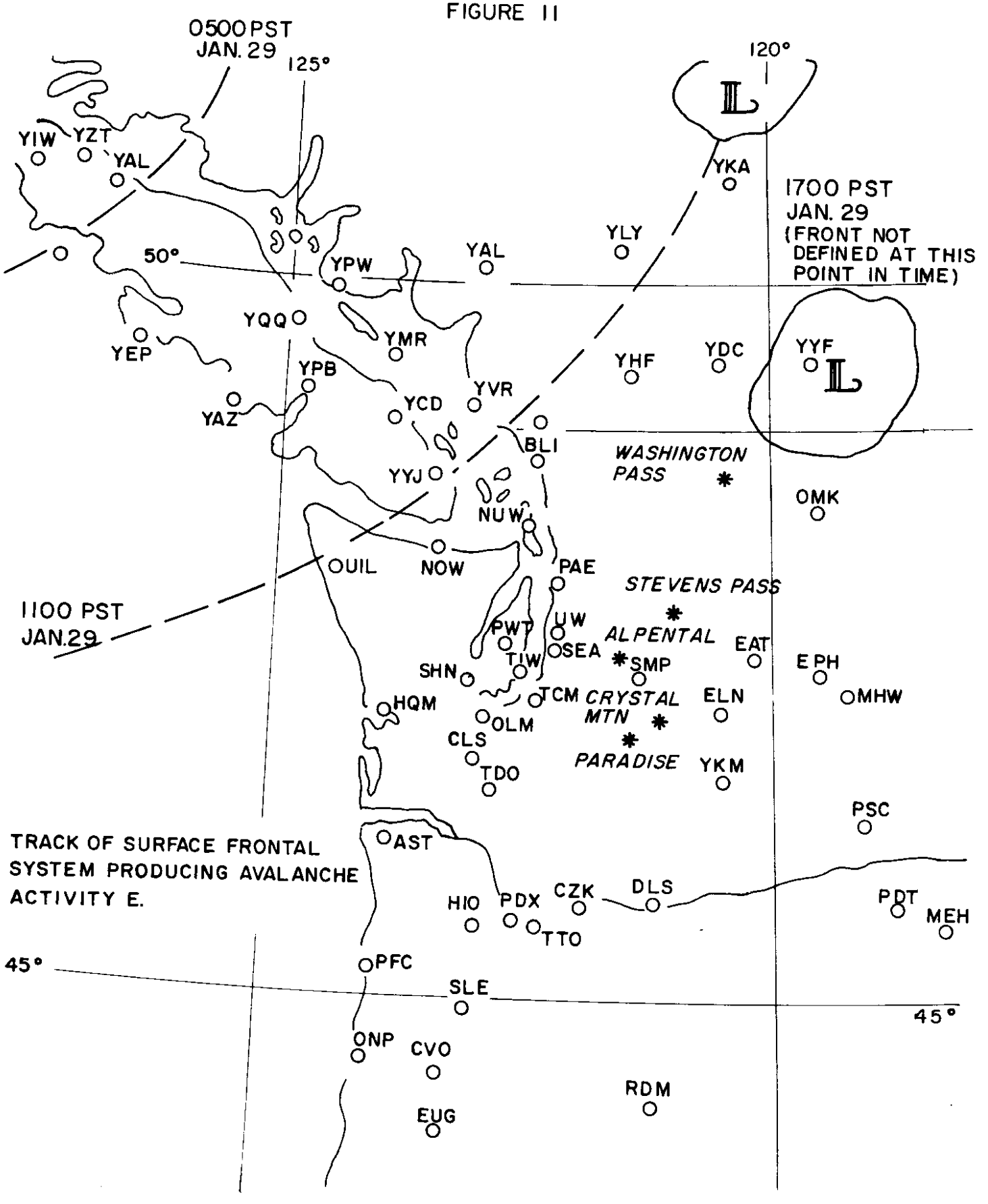
0500 PST
JAN. 29
125°
120°
YIW
YZT
YAL
YKA
1700 PST
JAN. 29
(FRONT NOT
DEFINED AT THIS
POINT IN TIME)
YLY
50°
YPW
YAL
YQQ
YMR
YEP
YPB
YHF
YDC
YYF
YAZ
YCD
YVR
BLI
WASHINGTON
PASS
YYJ
OMK
NUW
OUIL
NOW
PAE
STEVENS PASS
1100 PST
JAN.29
PWT
UW
ALPENTAL
EAT
SEA
SMP
EPH
SHN
TIW
TCM
CRYSTAL
MTN
ELN
MHW
HQM
OLM
CLS
PARADISE
YKM
TDO
PSC
TRACK OF SURFACE FRONTAL
SYSTEM PRODUCING AVALANCHE
ACTIVITY E.
AST
HIO
PDX
CZK
DLS
PDT
MEH
TTO
45°
PFC
SLE
45°
ONP
CVO
RDM
EUG

FIGURE 12

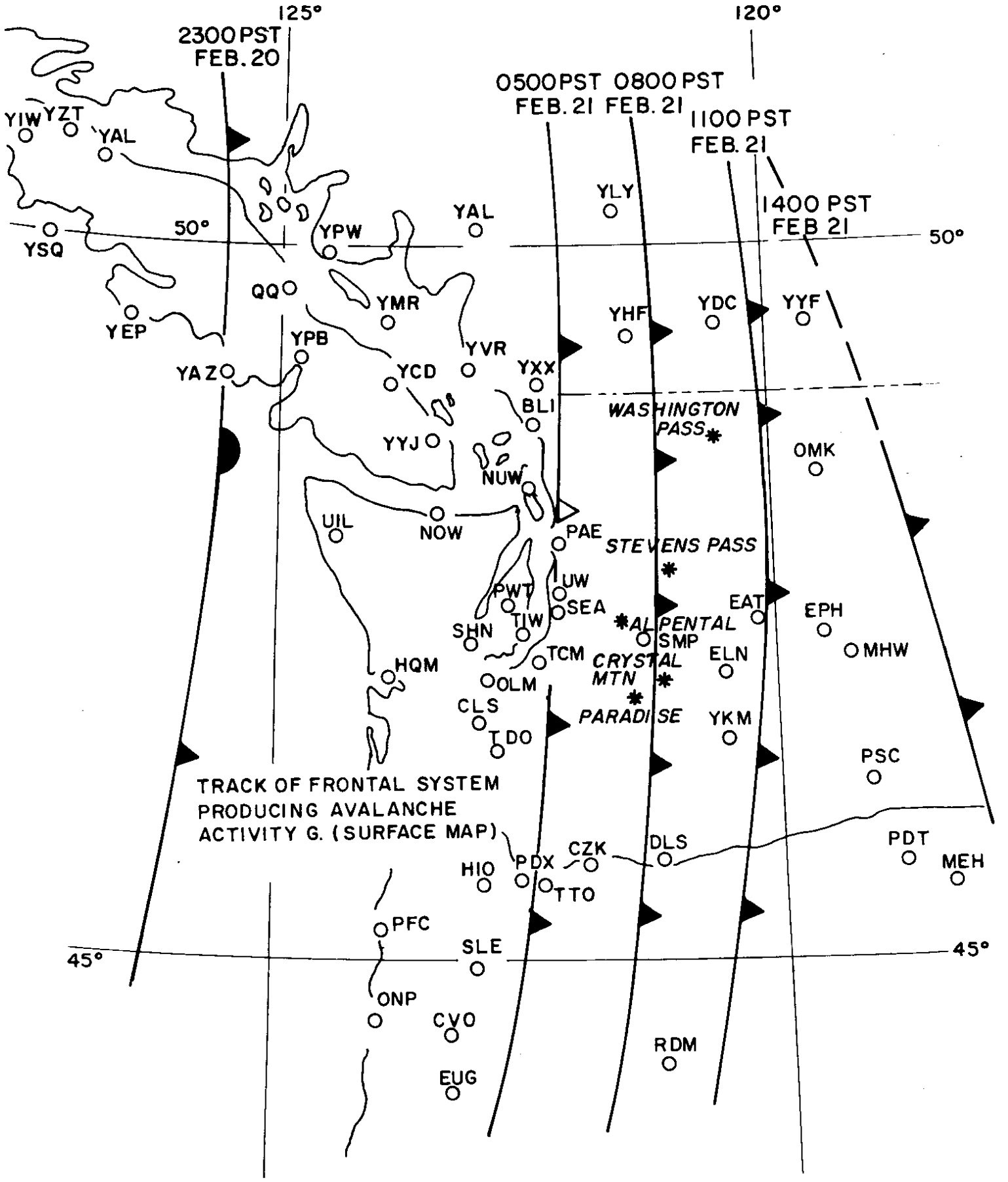
125°
120°
2300 PST FEB. 20
0500 PST FEB. 21
0800 PST FEB. 21
1100 PST FEB. 21
1400 PST FEB 21
50°
45°
YIW
YZT
YAL
YSQ
YPW
YEP
QQ
YMR
YPB
YAZ
YCD
YVR
YXX
YLY
YHF
YDC
YYF
BLI
YYJ
NUW
UIL
NOW
PAE
WASHINGTON PASS
OMK
STEVENS PASS
UW
PWT
SEA
TIW
SHN
ALPENTAL
SMP
EAT
EPH
MHW
ELN
TCM
CRYSTAL MTN
HQM
OLM
CLS
PARADISE
YKM
TDO
PSC
TRACK OF FRONTAL SYSTEM PRODUCING AVALANCHE ACTIVITY G. (SURFACE MAP)
PDT
MEH
DLS
CZK
PDX
HIO
TTO
PFC
SLE
ONP
CVO
RDM
EUG

FIGURE 13

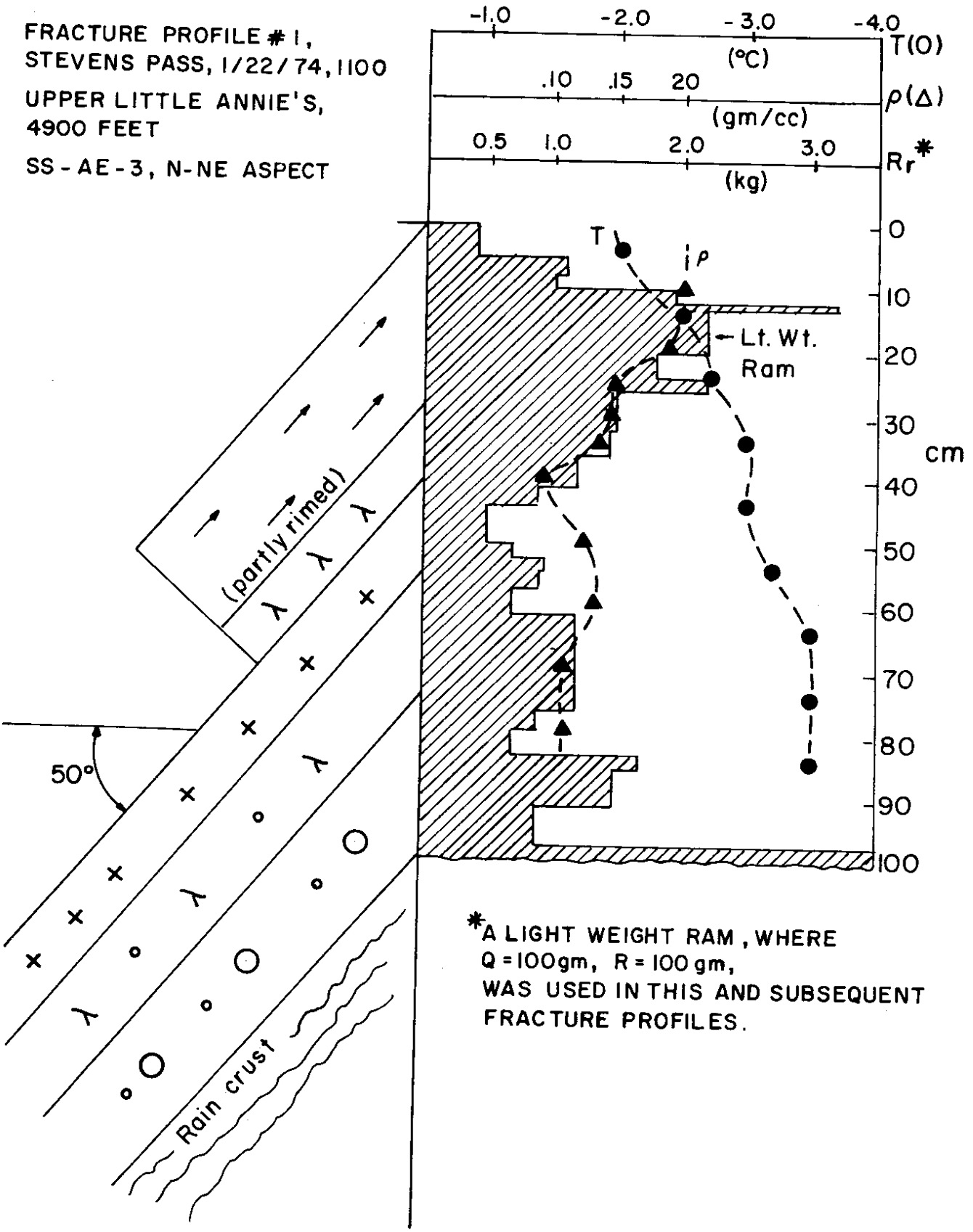
FRACTURE PROFILE # 1,
STEVENS PASS, 1/22/74, 1100
UPPER LITTLE ANNIE'S,
4900 FEET
SS - AE - 3, N-NE ASPECT
-1.0
-2.0
-3.0
-4.0
T(0)
(°C)
.10
.15
20
ρ(Δ)
(gm/cc)
0.5
1.0
2.0
3.0
Rr*
(kg)
T
ρ
Lt. Wt.
Ram
0
10
20
30
40
50
60
70
80
90
100
cm
(partly rimed)
50°
Rain crust
*A LIGHT WEIGHT RAM, WHERE
Q = 100 gm, R = 100 gm,
WAS USED IN THIS AND SUBSEQUENT
FRACTURE PROFILES.

FIGURE 14

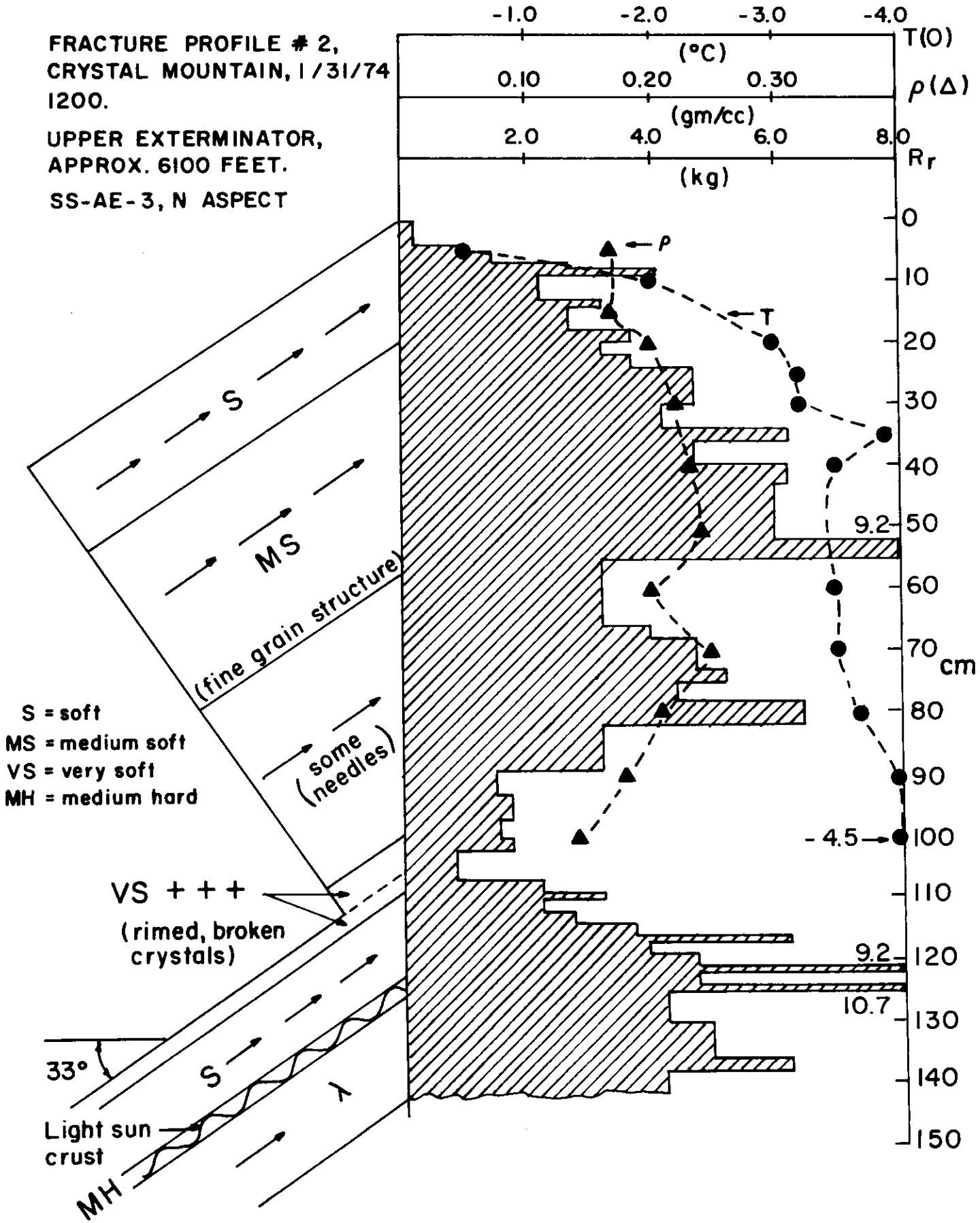
FRACTURE PROFILE # 2,
CRYSTAL MOUNTAIN, 1/31/74
1200.
UPPER EXTERMINATOR,
APPROX. 6100 FEET.
SS-AE-3, N ASPECT
-1.0
-2.0
-3.0
-4.0
T(0)
(°C)
0.10
0.20
0.30
ρ(Δ)
(gm/cc)
2.0
4.0
6.0
8.0
Rr
(kg)
ρ
T
S
MS
(fine grain structure)
(some needles)
VS + + +
(rimed, broken crystals)
S
λ
33°
Light sun crust
MH
S = soft
MS = medium soft
VS = very soft
MH = medium hard
9.2
-4.5
9.2
10.7
0
10
20
30
40
50
60
70
cm
80
90
100
110
120
130
140
150